

Optomechanics and quantum measurement

Aashish A. Clerk

Department of Physics, McGill University, Montréal, Québec, Canada H3A 2T8

OXFORD
UNIVERSITY PRESS

Contents

1	Introduction	1
2	Basic quantum cavity optomechanics theory	2
2.1	Optomechanical Hamiltonian	2
2.2	Dissipation and noise	3
2.3	Driving and output field	5
2.4	Displacement transformation	6
2.5	Linearized regime of optomechanics	7
3	Quantum limit on continuous position detection	10
3.1	General problem: minimizing total detector added noise	10
3.2	Quantum noise spectral densities: some essential features	12
3.3	Heisenberg inequality on detector quantum noise	16
3.4	Power gain and the large gain limit	20
3.5	Defining the quantum limit	21
3.6	Derivation of the quantum limit	24
3.7	Simple limits and discussion	26
3.8	Applications to an optomechanical cavity (with and without input squeezing)	28
4	Backaction evasion and conditional squeezing	33
4.1	Single quadrature measurements	33
4.2	Two-tone QND scheme	34
4.3	Conditional squeezing: heuristic description	38
4.4	Stochastic master equation description of a conditional measurement	39
4.5	Conditional back-action evading measurement	44
4.6	Feedback to create unconditional squeezing	46
4.7	Extensions of back-action evasion techniques	47
	Appendix A Derivation of power gain expression	48
	References	51

1

Introduction

These notes summarize lectures given at the 2015 Les Houches School on Optomechanics. The first part of the notes give a quick review of the basic theory of quantum optomechanical systems, based largely on linearized Heisenberg-Langevin equations. The notes then focus on selected topics relating to quantum measurement and quantum optomechanics. Chapter 3 gives comprehensive discussion of the quantum limit on the added noise of a continuous position detector, following the quantum linear response approach. While much of this discussion can already be found in (Clerk, 2004; Clerk *et al.*, 2010), I provide a greater discussion here of the role of noise correlations, and how these can be achieved in an optomechanical cavity (by using squeezed input light, or by modifying the choice of measured output quadrature). Chapter 4 turns to a discussion of back-action evading measurements of a mechanical quadrature, discussing how this can be achieved in a two-tone driven cavity system. I also provide a quick introduction to the theory of conditional continuous quantum measurement, and use it to discuss how a back-action evading measurement can be used to produce conditional mechanical squeezed states.

2

Basic quantum cavity optomechanics theory

This chapter will present a “quick and dirty” introduction to the basic theoretical language used to describe quantum optomechanical systems. More complete introductions to some of the topics covered here can be found in (Clerk *et al.*, 2010; Aspelmeyer *et al.*, 2014; Clerk and Marquardt, 2014)

2.1 Optomechanical Hamiltonian

We start by considering a standard optomechanical system, consisting of a single mode of a resonant electromagnetic cavity whose frequency ω_{cav} depends on the position x of a mechanical resonator. Both the mechanical mode and cavity mode are harmonic oscillators, and the Hamiltonian takes the form ($\hbar = 1$):

$$\hat{H}_{\text{OM}} = \omega_{\text{cav}}[\hat{x}]\hat{a}^\dagger\hat{a} + \omega_M\hat{b}^\dagger\hat{b} \quad (2.1)$$

where \hat{a} is the annihilation operator for the cavity mode, \hat{b} is the annihilation operator for the mechanical mode. Finally, as we are typically interested in small mechanical displacements, we can Taylor expand the dependence of ω_{cav} on x keeping just the first term. Writing the mechanical position in terms of creation and destruction operators, the optomechanical Hamiltonian takes the form:

$$\hat{H}_{\text{OM}} = \omega_{\text{cav}}\hat{a}^\dagger\hat{a} + \omega_M\hat{b}^\dagger\hat{b} + g\hat{a}^\dagger\hat{a}(\hat{b} + \hat{b}^\dagger) \equiv \hat{H}_0 + \hat{H}_{\text{int}} \quad (2.2)$$

where

$$g = \frac{d\omega_{\text{cav}}}{dx}x_{\text{ZPF}} = \frac{d\omega_{\text{cav}}}{dx}\sqrt{\frac{\hbar}{2m\omega_M}}. \quad (2.3)$$

It is worth noting a few basic features of this Hamiltonian:

- The position x of the mechanical resonator sets the cavity frequency; thus, if you drive the cavity with a monochromatic laser, the average cavity photon number $\langle\hat{a}^\dagger\hat{a}\rangle$ will also depend on the mechanical position.
- Anything that multiplies \hat{x} in a Hamiltonian acts as a force on the mechanical resonator. Hence, the cavity photon number $\hat{n} = \hat{a}^\dagger\hat{a}$ is a force on the mechanical resonator (i.e. the radiation pressure force).
- Without loss of generality, we have defined the optomechanical interaction with a plus sign in this chapter. Hence, a positive displacement $x > 0$ of the mechanics

results in an increased cavity frequency. We also use g to denote the single-photon optomechanical coupling strength in this chapter (the same quantity which is denoted g_0 in other works, e.g. (Aspelmeyer *et al.*, 2014)).

A rigorous derivation of this Hamiltonian (for the specific case of a Fabry-Perot resonator with a moveable end mirror) was given in (Law, 1995). This derivation keeps all the resonant modes of the optical cavity, and shows how in principle one also obtains interaction terms where the mechanical resonator can mediate scattering between different optical modes, and also terms corresponding to the dynamical Casimir effect, where, e.g. , destruction of a phonon can result in the creation of a pair of photons. Such additional terms are of negligible importance in the standard situation where the mechanical frequency ω_M is much smaller than all optical frequency scales.

Returning to the basic Hamiltonian \hat{H}_{OM} above, one sees immediately that the cavity photon number \hat{n} commutes with \hat{H} and is thus a conserved quantity. Thus, in the absence of any driving or coupling to dissipation, \hat{H}_{OM} can easily be exactly diagonalized. For a fixed photon number, the optomechanical interaction corresponds to a static force on the mechanics, which simply shifts its equilibrium position an amount $\Delta x_n = -2(g/\omega_M)x_{\text{ZPF}}$. The eigenstates are just tensor products of states of fixed photon number with displaced harmonic oscillator eigenstates. This is conveniently described by making a polaron transformation, i.e. a \hat{n} -dependent displacement transformation of the mechanical resonator:

$$\hat{U} = \exp(-i\hat{p}\Delta x_n) = \exp\left(\frac{g}{\omega_M}\hat{n}(\hat{b} - \hat{b}^\dagger)\right) \quad (2.4)$$

The transformed Hamiltonian takes the form:

$$\hat{U}^\dagger \hat{H}_{\text{OM}} \hat{U} = \left(\omega_{\text{cav}} - \frac{g^2}{\omega_M}\right) \hat{a}^\dagger \hat{a} + \omega_M \hat{b}^\dagger \hat{b} - \frac{g^2}{\omega_m} \hat{a}^\dagger \hat{a}^\dagger \hat{a} \hat{a} \quad (2.5)$$

In this new frame, we see explicitly from the last term that the eigenenergies of the Hamiltonian have a nonlinear dependence on photon number: the mechanical resonator mediates an optical Kerr-type nonlinearity (or equivalently, photon-photon interaction). In the simplest picture, we simply combine the two features noted above: as ω_{cav} depends on x , and x depends on \hat{n} (as it is a force), the cavity frequency will depend on \hat{n} . This yields the \hat{n}^2 term above. In a more quantum picture, note that to leading order, the interaction \hat{H}_{int} creates or destroys a mechanical excitation (a phonon) with a matrix element proportional to \hat{n} . While such a process would not conserve energy, to second order we could have an energy conserving process that involves a virtual state with a mechanical excitation. The amplitude of such a process would be proportional to \hat{n}^2 and inversely proportional to ω_M (i.e. the energy cost of the virtual state). This is yet another way to understand the last term in Eq. (2.5).

2.2 Dissipation and noise

Next, we need to include the coupling of both the cavity and the mechanical resonator to their respective dissipative environments, as well any driving terms (e.g. a coherent laser drive of the cavity). We follow the standard input-output theory route to treat

4 Basic quantum cavity optomechanics theory

these effects (see, e.g. (Walls and Milburn, 2008; Clerk *et al.*, 2010)), where the cavity mode (mechanical mode) acquires an energy damping rate κ (γ). To obtain these effects, one needs to include terms in the Hamiltonian describing the dissipative baths and their coupling to the system:

$$\hat{H} = \hat{H}_{\text{OM}} + \hat{H}_\kappa + \hat{H}_\gamma \quad (2.6)$$

Consider first the cavity dissipation, described by \hat{H}_κ . This just describes a linear coupling between the cavity mode and extra-cavity photon modes, which are themselves just free bosons (lowering operators \hat{b}_q):

$$\hat{H}_\kappa = \sum_q \omega_q \hat{b}_q^\dagger \hat{b}_q - i \sqrt{\frac{\kappa}{2\pi\rho}} \sum_q \left(\hat{a}^\dagger \hat{b}_q - h.c. \right) \quad (2.7)$$

As is standard, we approximate the bath density of states to be a frequency-independent constant (which is typically an excellent approximation, as we are only interested in a small range of bath frequencies centred around the cavity frequency ω_{cav}):

$$\sum_q \delta(\omega - \omega_q) = \rho \quad (2.8)$$

As described in, e.g. (Clerk *et al.*, 2010), one can now derive the effective Heisenberg-Langevin equation of motion for the cavity field. This involves first solving the Heisenberg equation of motion for the bath operators \hat{b}_q , and then substituting these into the Heisenberg equation of motion for the cavity mode lowering operator \hat{a} . One obtains:

$$\frac{d}{dt} \hat{a} = -i \left[\hat{a}, \hat{H}_{\text{OM}} \right] - \frac{\kappa}{2} \hat{a} - \sqrt{\kappa} \hat{a}_{\text{in}} \quad (2.9)$$

The second term on the RHS describes the a simple linear damping of the cavity (resulting from photons leaking from the cavity to the bath), while the third term describes a driving of the cavity mode by noise emanating from the bath. Note that \hat{a}_{in} has been normalized so that $\hat{a}_{\text{in}}^\dagger \hat{a}_{\text{in}}$ represents a photon number flux (i.e. \hat{a}_{in} has units of $1/\sqrt{\text{time}}$).

Taking the bath to be in a thermal equilibrium state, one finds that the operator-valued input noise $\hat{a}_{\text{in}}(t)$ is Gaussian (i.e. fully characterized by two-point correlation functions). Further, for the typically small frequency scales of interest, it can also be approximated as being white noise. One obtains:

$$\langle \hat{a}_{\text{in}}(t) \hat{a}_{\text{in}}^\dagger(t') \rangle = \delta(t - t') (1 + \bar{n}_{\text{th}}^c) \quad (2.10)$$

$$\langle \hat{a}_{\text{in}}^\dagger(t) \hat{a}_{\text{in}}(t') \rangle = \delta(t - t') \bar{n}_{\text{th}}^c \quad (2.11)$$

Here, $\bar{n}_{\text{th}}^{\text{cav}}$ is a Bose-Einstein occupancy factor evaluated at the cavity frequency and at the bath temperature. Note that the input noise satisfies the canonical commutation relation

$$\left[\hat{a}_{\text{in}}(t), \hat{a}_{\text{in}}^\dagger(t') \right] = \delta(t - t') \quad (2.12)$$

One can treat the effects of mechanical dissipation in a completely analogous manner. The Heisenberg-Langevin equation of motion for the mechanical lowering operator takes the form

$$\frac{d}{dt}\hat{b} = -i\left[\hat{b}, \hat{H}_{\text{OM}}\right] - \frac{\gamma}{2}\hat{b} - \sqrt{\kappa}\hat{b}_{\text{in}} \quad (2.13)$$

The mechanical input noise has correlation functions analogous to those in Eqs. (2.10),(2.11), except that $\bar{n}_{\text{th}}^{\text{cav}}$ is replaced by $\bar{n}_{\text{th}}^{\text{M}}$, a Bose-Einstein factor evaluated at the mechanical frequency and mechanical bath temperature.

Finally, we note that the approximations we have made in treating the bath (i.e. taking it to have a constant density of states, and taking its noise correlation functions to be delta-correlated) correspond to treating it as a Markovian bath (a vanishing correlation time, absence of memory effects). The resulting Heisenberg-Langevin equations are completely local in time.

2.3 Driving and output field

To include a coherent driving of the cavity (e.g. by a laser), we simply allow the input field \hat{a}_{in} to have an average value $\bar{a}_{\text{in}}(t)$. One can easily confirm that this is completely equivalent to having added an explicit linear driving term

$$\hat{H}_{\text{drive}} = -i(\bar{a}_{\text{in}}(t)\hat{a}^\dagger - h.c.) \quad (2.14)$$

to the Hamiltonian. In many cases, the cavity bath corresponds to modes in the waveguide (or transmission line) used to drive and measure the cavity. In this case, we are also interested in knowing what the field emitted by the cavity into the waveguide is. The amplitude of this outgoing field is described by the operator $\hat{a}_{\text{out}}(t)$. In the simple Markovian limit we are focusing on, this field is completely determined by the input-output relation:

$$\hat{a}_{\text{out}}(t) = \hat{a}_{\text{in}}(t) + \sqrt{\kappa}\hat{a}(t) \quad (2.15)$$

where the intra-cavity field \hat{a} is determined by the Heisenberg-Langevin equation Eq. (2.9). Note that $\hat{a}(t)$ is driven by the input field $\hat{a}_{\text{in}}(t)$, and hence the two terms on the RHS here are not independent. When $\kappa = 0$ (i.e. no coupling between the waveguide and the cavity), the input-output equation just describes a perfect reflection of waves off the end of the waveguide. For non-zero κ , the first term describes incident waves that are immediately reflected from the cavity-waveguide boundary, whereas the second term describes wave emitted from the waveguide.

Consider the simple case where we have a monochromatic coherent driving of the cavity: $\bar{a}_{\text{in}}(t) = \alpha_{\text{in}}e^{-i\omega_L t}$. It is convenient to work in a rotating frame where this driving looks time-independent. This is achieved by using the unitary $\hat{U}(t) = \exp(i\omega_L \hat{a}^\dagger \hat{a} t)$ to transform to a new frame. In this new frame, the Hamiltonian is given by ¹:

¹One also needs in principle to shift the frequency of the bath oscillators \hat{b}_q to make sure that in the new frame, the cavity-bath coupling remains time-independent. While this is normally innocuous, it does imply the presence of negative-frequency bath modes in the new frame. The implications of this for a driven optomechanical system are discussed in detail in (Lemondé and Clerk, 2015).

6 Basic quantum cavity optomechanics theory

$$\hat{H}' = \hat{U}(t)\hat{H}\hat{U}^\dagger(t) + i\left(\frac{d}{dt}\hat{U}(t)\right)\hat{U}^\dagger(t) \quad (2.16)$$

and the Heisenberg Langevin equation takes the form:

$$\frac{d}{dt}\hat{a} = -i\left[\hat{a}, -\Delta\hat{a}^\dagger\hat{a} + \omega_M\hat{b}^\dagger\hat{b} + \hat{H}_{\text{int}}\right] - \frac{\kappa}{2}\hat{a} - \sqrt{\kappa}\alpha_{\text{in}} - \sqrt{\kappa}\hat{a}_{\text{in}} \quad (2.17)$$

where the drive detuning $\Delta \equiv \omega_L - \omega_{\text{cav}}$, and we have explicitly separated out the average value of \hat{a}_{in} . Note that the RHS has no explicit time dependence.

In the case where there is no optomechanical coupling, one can easily solve the above equation for the stationary value of \hat{a} ; one finds:

$$\langle\hat{a}\rangle = -\frac{\sqrt{\kappa}\alpha_{\text{in}}}{\frac{\kappa}{2} - i\Delta} \equiv \alpha \quad (2.18)$$

It thus follows from Eq. (2.15) that the average output field is given by:

$$\langle\hat{a}_{\text{out}}\rangle = -\frac{\frac{\kappa}{2} + i\Delta}{\frac{\kappa}{2} - i\Delta}\alpha_{\text{in}} \equiv e^{i\theta}\alpha_{\text{in}} \quad (2.19)$$

We thus recover the expected expression for the reflection phase θ .

2.4 Displacement transformation

Let's now include the optomechanical interaction in Eq. (2.17). We expect again that the cavity drive will induce an average value for the cavity field \hat{a} , and will also induce an average value for the mechanical lowering operator \hat{b} (as the average photon number of the cavity is a static force on the mechanical resonator, which will displace its equilibrium position). It is useful to make displacement transformations to separate out these classical mean values from the additional dynamics that arises due to the noise operator \hat{a}_{in} and \hat{b}_{in} (operators which encode both classical and quantum noise driving the system). We thus introduce displaced cavity and mechanical lowering operators \hat{d} and \hat{b}_{new} defined via:

$$\hat{a} = \bar{a}_{\text{cl}} + \hat{d} \quad \hat{b} = \bar{b}_{\text{cl}} + \hat{b}_{\text{new}} \quad (2.20)$$

where $\bar{a}_{\text{cl}}, \bar{b}_{\text{cl}}$ are the classical average values for the cavity and mechanical mode operators. These are found by solving the classical, noise-free version of the Heisenberg-Langevin equations Eq. (2.9) and (2.13) (i.e. one replaces $\hat{a} \rightarrow \bar{a}_{\text{cl}}, \hat{b} \rightarrow \bar{b}_{\text{cl}}$ in the equations and drops all noise terms). These classical equations are nonlinear, and regimes exist where multiple classical solutions can be found (the well-known optomechanical bistability, see Sec. V.A of (Aspelmeyer *et al.*, 2014) for a discussion). We assume however that we work in a regime where there is a unique solution to the classical equations. As \hat{d} and \hat{b}_{new} encode all quantum effects in our system, it is common to refer to them as the quantum parts of the cavity and mechanical annihilation operators. We stress that they are standard canonical bosonic annihilation operators.

Once the classical amplitudes have been found, one returns to the full Heisenberg-Langevin equations, expressed now in terms of the operators \hat{d} and \hat{b}_{new} . One finds that

there are no purely constant terms on the RHS of these equations (i.e. linear driving terms). In particular, the coherent cavity drive α_{in} enters only through the classical displacements $\bar{a}_{\text{cl}}, \bar{b}_{\text{cl}}$. The resulting equations are equivalent to having started with a coherent Hamiltonian

$$\hat{H}_{\text{OM}} = -\Delta' \hat{d}^\dagger \hat{d} + \omega_M \hat{b}_{\text{new}}^\dagger \hat{b}_{\text{new}} + \hat{H}_{\text{int}} \quad (2.21)$$

$$\hat{H}_{\text{int}} = g \left(\bar{a}_{\text{cl}}^* \hat{d} + \bar{a}_{\text{cl}} \hat{d}^\dagger + \hat{d}^\dagger \hat{d} \right) \left(\hat{b}_{\text{new}}^\dagger + \hat{b}_{\text{new}} \right) \quad (2.22)$$

where the modified detuning $\Delta' = \Delta - g(\bar{b}_{\text{cl}} + \bar{b}_{\text{cl}}^*)$. We see than in this new displaced frame, the mechanical mode only interacts with the fluctuating parts of the cavity photon number \hat{n} (i.e. terms involving \hat{d}, \hat{d}^\dagger). Note that the static, ‘‘classical’’ part of the photon number $|\bar{a}_{\text{cl}}|^2$ determines the classical mechanical displacement \hat{b}_{cl} , but does not appear explicitly in \hat{H}_{OM} . In what follows, we drop the subscript ‘‘new’’ on \hat{b}_{new} to keep things clear, and also replace Δ' by Δ .

2.5 Linearized regime of optomechanics

By strongly driving the cavity (large α_{in}), \bar{a}_{cl} increases in magnitude. This in turn increases the fluctuations in the intracavity photon number, namely the term that is *linear* in the \hat{d} operators. Correspondingly (as per Eq. (2.22)), the large drive enhances the quadratic terms in the optomechanical interaction Hamiltonian. It is thus common to introduce a drive enhanced many-photon optomechanical interaction strength, defined as ²

$$G \equiv g |\bar{a}_{\text{cl}}| = g \sqrt{\bar{n}_{\text{cav}}} \quad (2.23)$$

In almost all current experiments, the single photon strength g is too weak to directly play a role (i.e. $g \ll \kappa, \omega_M$), and appreciable optomechanical effects are only obtained when the cavity is strongly driven and G made large. In this regime where $G \gg g$, it a good approximation to only retain the drive-enhanced terms in Eq. (2.22). The physics is then described by the approximate quadratic Hamiltonian:

$$\hat{H}_{\text{lin}} = -\Delta \hat{d}^\dagger \hat{d} + \omega_M \hat{b}^\dagger \hat{b} + G(\hat{b} + \hat{b}^\dagger)(\hat{d} + \hat{d}^\dagger) \quad (2.24)$$

with corresponding Heisenberg-Langevin equations:

$$\frac{d}{dt} \hat{d} = (i\Delta - \kappa/2) \hat{d} - iG(\hat{b} + \hat{b}^\dagger) - \sqrt{\kappa} \hat{d}_{\text{in}} \quad (2.25)$$

$$\frac{d}{dt} \hat{b} = (-i\omega_M - \gamma/2) \hat{b} - iG(\hat{d} + \hat{d}^\dagger) - \sqrt{\gamma} \hat{b}_{\text{in}} \quad (2.26)$$

Note that we have made a gauge transformation on the cavity field to absorb the phase of the classical cavity field \bar{a}_{cl} . In this regime, the equations of motion for the cavity and mechanical lowering operators are purely linear, and thus it is often termed

²It is also common notation to use g_0 (instead of g) to denote the single-photon optomechanical coupling strength, and use g (instead of G) to denote the many-photon coupling strength. We prefer the notation used here, both as it avoids having to use yet another subscript, and because the use of a capital letter more dramatically emphasizes the coupling enhancement by the drive.

the linearized regime of optomechanics. The physics is just that of a system of two linearly coupled harmonic oscillators, albeit one with a great deal of tunability, and one where the dissipative rates and effective temperatures of the two oscillators can be very different. The effective frequency of the photonic oscillator can be tuned by changing the frequency of the cavity drive, and the strength of the interaction G can be tuned by changing the amplitude of the cavity drive.

To get a feel for the various interesting things that can be done with linearized optomechanics, we quickly sketch different interesting possibilities below.

2.5.1 Beam-splitter Hamiltonian

Consider Eq. (2.27) in the regime where $\Delta = -\omega_M$, implying that the cavity drive frequency is detuned to the red of the cavity resonance an amount exactly equal to the mechanical frequency (a so-called red-sideband drive). The two effective oscillators in Eq. (2.27) are then resonant. If we further assume that $\omega_M \gg \kappa$ and that $G \ll \omega_M$, the interaction terms that create or destroy a photon-phonon pair are sufficiently non-resonant to not play a large role in the dynamics. We can thus make a rotating wave approximation, keeping only the energy conserving interaction terms. The Hamiltonian then takes the simple form:

$$\hat{H}_{\text{lin}} = -\Delta \hat{d}^\dagger \hat{d} + \omega_M \hat{b}^\dagger \hat{b} + G(\hat{b}^\dagger \hat{d} + \hat{d}^\dagger \hat{b}) \quad (2.27)$$

This interaction converts photons to phonons and vice-versa, and is known as a beam-splitter Hamiltonian or “swap” Hamiltonian. It is at the heart of quantum state-transfer applications of optomechanics (see, e.g., (Hill *et al.*, 2012; Dong *et al.*, 2012; Andrews *et al.*, 2014)). It also is at the heart of optimal cavity-cooling schemes, where one uses the driven cavity to cool a thermal mechanical resonator to close to the ground state (Marquardt *et al.*, 2007; Wilson-Rae *et al.*, 2007). The above swap-Hamiltonian can be used to transfer mechanical excitations to the cavity mode, where they are quickly emitted (at a rate κ) to the cavity bath.

2.5.2 Entangling Hamiltonian

Consider Eq. (2.27) for the opposite detuning choice, where $\Delta = \omega_M$: the cavity drive frequency is now detuned to the blue of the cavity resonance an amount ω_M . If we again assume that the good-cavity condition $\omega_M \gg \kappa$ is fulfilled and that $G \ll \omega_M$, we can again make a rotating-wave approximation where we only retain energy conserving terms. As now the cavity photons have an effective negative frequency, the energy conserving terms correspond to creating or destroying pairs of excitations, and the Hamiltonian becomes:

$$\hat{H}_{\text{lin}} = -\omega_M \hat{d}^\dagger \hat{d} + \omega_M \hat{b}^\dagger \hat{b} + G(\hat{b}^\dagger \hat{d}^\dagger + \hat{d} \hat{b}) \quad (2.28)$$

The dynamics of this Hamiltonian creates photons and phonons in pairs, and leads to states with a high degree of correlations between the mechanics and light (i.e. the photon number and phonon number are almost perfectly correlated). Such states are known as “two-mode squeezed states”, and their correlations correspond to quantum entanglement. Such optomechanical entanglement has recently been measured. The

above Hamiltonian also corresponds to the Hamiltonian of a non-degenerate parametric amplifier. It can be used for near quantum-limited amplification. It also can exhibit dynamical instabilities for sufficiently large values of G .

3

Quantum limit on continuous position detection

One of the key motivations for studying optomechanics is the possibility to use light to measure mechanical motion with a precision limited by the fundamental constraints imposed by quantum mechanics. In some cases, one can even devise schemes that transcend the quantum constraints that limit more conventional measurement strategies. In this chapter, we will review the most general and rigorous formulation of the quantum limit on continuous position detection for a generic linear-response detector. The general derivation will make the origin of this quantum limit clear, as well establish a set of requirements which must be met to achieve it. We will then apply this general formalism to the basic optomechanical cavity as introduced in the previous chapter. The presentation here is closely related to that developed in (Clerk, 2004) and (Clerk *et al.*, 2010). In contrast to those works, we provide a discussion of how squeezing can be used to generate the noise correlations needed to reach the quantum limit in the free mass limit.

3.1 General problem: minimizing total detector added noise

To motivate things, let's return to Eq. (2.19) for the reflection phase shift for a driven single-sided cavity, and give a classical discussion of how our cavity could function as a position detector. For a fixed cavity drive frequency, the reflection phase shift θ is a function of the cavity frequency ω_{cav} . With the optomechanical coupling, the instantaneous cavity frequency becomes a function of the mechanical position. Consider first the simple case where x is fixed to some unknown position x_0 . The mechanical displacement shifts the cavity frequency by an amount gx_0/x_{ZPF} . For small displacements, the change in phase will be linear in x_0 . In the optimal case where $\Delta = 0$, we have

$$\theta = \pi + \frac{4g}{\kappa} \frac{x_0}{x_{\text{ZPF}}} \equiv \theta_0 + \Delta\theta \quad (3.1)$$

(with $\theta_0 = \pi$) and the output field from the cavity will have the form

$$a_{\text{out}} = e^{i(\theta_0 + \Delta\theta)} a_{\text{in}} \simeq e^{i\theta_0} (1 + i\Delta\theta) a_{\text{in}} = -(1 + i\Delta\theta) a_{\text{in}} \quad (3.2)$$

where a_{in} is the amplitude of the incident cavity driving field. Information on the mechanical displacement x_0 is encoded in the change in reflection phase $\Delta\theta$, and

will thus be optimally contained in the phase quadrature of the output field. Taking (without loss of generality) a_{in} to be real, this quadrature is defined as:

$$X_\phi(t) = -i(a_{\text{out}}(t) - a_{\text{out}}^*(t)) \quad (3.3)$$

Using the standard technique of homodyne interferometry, this output-field quadrature can be directly converted into a photocurrent $I(t) \propto X_\phi$ (see e.g. (Walls and Milburn, 2008; Clerk *et al.*, 2010)). This photocurrent will have intrinsic fluctuations (due to shot noise in the light), and hence will have the form:

$$I(t) = \lambda x_0 + \delta I_0(t) \quad (3.4)$$

The first term is the “signal” associated with the measurement, where $\lambda \propto g$ parameterizes the response of the photocurrent to changes in position. The second term represents the imprecision noise in the measurement, i.e. the intrinsic fluctuations in the photocurrent. At each instant t , $\delta I_0(t)$ is a random variable with zero mean. To determine x_0 , one would need to integrate $I(t)$ over some finite time interval to resolve the signal above these intrinsic fluctuations. It is common to scale these intrinsic output fluctuations by the response coefficient λ , and think of this noise as an equivalent mechanical position noise $\delta x_{\text{imp}}(t) \equiv \delta I_0(t)/\lambda$.

If the mechanical resonator is now in motion, and ω_M is sufficiently small (i.e. much smaller than κ), then the cavity will be able to adiabatically follow the mechanical motion. Eq. (3.4) will then still hold, with the replacement $x_0 \rightarrow x_0(t)$. Our goal here will not be to measure the instantaneous position of the mechanical resonator: we consider the standard situation where the mechanical resonator is in motion (oscillating!), and the optomechanical coupling is far too weak to measure position in a time short compared to the mechanical period. Instead, our goal will be to determine the quadrature amplitudes describing the oscillating motion, i.e. the amplitudes of the sine and cosine components of the motion:

$$x(t) = X(t) \cos(\Omega t) + Y(t) \sin(\Omega t). \quad (3.5)$$

These amplitudes typically evolve on a time scale much longer than the mechanical period.

One might think that in principle, one could increase the signal-to-noise ratio indefinitely by increasing λ (e.g. by increasing g or the power associated with the cavity drive). From a quantum point of view, we know the situation cannot be that simple, as the quadrature amplitudes X and Y become non-commuting, conjugate observables, and cannot be known simultaneously with arbitrary precision. More concretely, in the quantum case, we absolutely need to think about an additional kind of measurement noise: the disturbance of the mechanical position by the detector, otherwise known as back-action. Returning to the optomechanical Hamiltonian of Eq. (2.2), we see that fluctuations of cavity photon number act like a noisy force on the mechanical resonator. This will give rise to extra fluctuations in its position, $\delta x_{\text{BA}}(t)$. Eq. (3.4) thus needs to be updated to have the form:

$$I(t) = \lambda [x_0(t) + \delta x_{\text{BA}}(t)] + \delta I_0(t) \equiv \lambda [x_0(t) + \delta x_{\text{add}}(t)] \quad (3.6)$$

We have introduced here the total added noise of the measurement $\delta x_{\text{add}}(t) = \delta x_{\text{BA}}(t) + \delta I_0(t)/\lambda$.

12 Quantum limit on continuous position detection

The goal is now to make this total added noise as small as possible, and to understand if there are any fundamental limits to its size. Simply increasing the coupling strength or optical power no longer is a good strategy: in this limit, the second “imprecision” noise term in $\delta x_{\text{add}}(t)$ will become negligible, but the first back-action term will be huge. Similarly, in the opposite limit where the coupling (or optical drive power) is extremely weak, back-action noise will be negligible, but the imprecision noise will be huge. Clearly, some trade-off between these two limits will be optimal. Further, one needs to consider whether these two kinds of noises (imprecision and back-action) can be correlated, and whether this is desirable.

Our goal in what follows will be to first review how one characterizes the magnitude of noise via a spectral density, and then to establish the rigorous quantum limit on how small one can make the added noise $\delta x_{\text{add}}(t)$.

3.2 Quantum noise spectral densities: some essential features

In this section, we give a compact (and no doubt highly incomplete) review of some basic properties of quantum noise spectral densities. We start however with the simpler case of spectral densities describing classical noise.

3.2.1 Classical noise basics

Consider a classical random signal $I(t)$. The signal is characterized by zero mean $\langle I(t) \rangle = 0$, and autocorrelation function

$$G_{II}(t, t') = \langle I(t)I(t') \rangle. \quad (3.7)$$

The autocorrelation function is analogous to a covariance matrix: for $t = t'$, it tells us the variance of the fluctuations of $I(t)$, where as for $t \neq t'$, it tells us if and how fluctuations of $I(t)$ are correlated with those at $I(t')$. Some crucial concepts regarding noise are:

- *Stationary noise.* The statistical properties of the fluctuations are time-translation invariant, and hence $G_{II}(t, t') = G_{II}(t - t')$.
- *Gaussian fluctuations.* The noise is fully characterized by its autocorrelation function; there are no higher-order cumulants.
- *Correlation time.* This time-scale τ_c governs the decay of $G_{II}(t)$: $I(t)$ and $I(t')$ are uncorrelated (i.e. $G_{II}(t - t') \rightarrow 0$) when $|t - t'| \gg \tau_c$.

For stationary noise, it is often most useful to think about the fluctuations in the frequency domain. In the same way that $I(t)$ is a Gaussian random variable with zero mean, so is its Fourier transform, which we define as:

$$I_T[\omega] = \frac{1}{\sqrt{T}} \int_{-T/2}^{+T/2} dt e^{i\omega t} I(t), \quad (3.8)$$

where T is the sampling time. In the limit $T \gg \tau_c$ the integral is a sum of a large number $N \approx \frac{T}{\tau_c}$ of random uncorrelated terms. We can think of the value of the integral as the end point of a random walk in the complex plane which starts at the origin. Because the distance traveled will scale with \sqrt{T} , our choice of normalization makes

the statistical properties of $I[\omega]$ independent of the sampling time T (for sufficiently large T). Notice that $I_T[\omega]$ has the peculiar units of $[I]\sqrt{\text{secs}}$ which is usually denoted $[I]/\sqrt{\text{Hz}}$.

The spectral density of the noise (or power spectrum) $\mathcal{S}_{II}[\omega]$ answers the question “how big is the noise at frequency ω ?”. It is simply the variance of $I_T(\omega)$ in the large-time limit:

$$\mathcal{S}_{II}[\omega] \equiv \lim_{T \rightarrow \infty} \langle |I_T[\omega]|^2 \rangle = \lim_{T \rightarrow \infty} \langle I_T[\omega] I_T[-\omega] \rangle. \quad (3.9)$$

A reasonably straightforward manipulation (known as the Wiener-Khinchin theorem) tells us that the spectral density is equal to the Fourier transform of the autocorrelation function

$$\mathcal{S}_{II}[\omega] = \int_{-\infty}^{+\infty} dt e^{i\omega t} G_{II}(t). \quad (3.10)$$

We stress that Eq. (3.9) provides a simple intuitive understanding of what a spectral density represents, whereas in theoretical calculations, one almost always starts with the expression in Eq. (3.10). We also stress that since the autocorrelation function $G_{II}(t)$ is real, $\mathcal{S}_{II}[\omega] = \mathcal{S}_{II}[-\omega]$. This is of course in keeping with Eq. (3.8), which tells us that negative and positive frequency components of the noise are related by complex conjugation, and hence necessarily have the same magnitude.

3.2.2 Definition of quantum noise spectral densities

In formulating quantum noise, one turns from a noisy classical signal $I(t)$ to a Heisenberg-picture Hermitian operator $\hat{I}(t)$. Similar to our noisy classical signal, one needs to think about measurements of $\hat{I}(t)$ statistically. One can thus introduce a quantum-noise spectral density which completely mimics the classical definition, e.g.:

$$S_{xx}[\omega] = \int_{-\infty}^{+\infty} dt e^{i\omega t} \langle \hat{x}(t) \hat{x}(0) \rangle. \quad (3.11)$$

We have simply inserted the quantum autocorrelation function in the classical definition. The expectation value is the quantum statistical average with respect to the noisy system’s density matrix; we assume that this is time-independent, which then also gives us an autocorrelation function which is time-translational invariant.

What makes quantum noise so quantum? There are at least three answers to this question:

- *Zero-point motion.* While a classical system at zero-temperature has no noise, quantum mechanically there are still fluctuations, i.e. $S_{xx}[\omega]$ need not be zero.
- *Frequency asymmetry.* Quantum mechanically, $\hat{x}(t)$ and $\hat{x}(t')$ need not commute when $t \neq t'$. As a result the autocorrelation function $\langle \hat{x}(t) \hat{x}(t') \rangle$ can be complex, and $S_{xx}[\omega]$ need not equal $S_{xx}[-\omega]$. This of course can never happen for a classical noise spectral density.
- *Heisenberg constraints.* For any system that can act as a detector or amplifier, there are fundamental quantum constraints that bound its noise. These constraints have their origin in the uncertainty principle, and have no classical counterpart.

3.2.3 Noise asymmetry and fluctuation dissipation theorem

The asymmetry in frequency of quantum noise spectral densities is a topic that is discussed in great detail in (Clerk *et al.*, 2010). In short, this asymmetry directly reflects the asymmetry in the noisy system's ability to absorb versus emit energy. This aspect of quantum noise spectral densities provides an extremely useful route to understanding optomechanical damping effects. While this asymmetry will not be the main focus of our discussion here, it is useful to consider a simple but instructive example which helps demystify two-sided quantum noise spectral densities. Consider a harmonic oscillator that is coupled weakly to a noise force produced by a second quantum system. This force is described by an operator \hat{F} , and the coupling to the harmonic oscillator is

$$\hat{H}_{\text{int}} = -\hat{x}\hat{F}. \quad (3.12)$$

Of course, the basic optomechanical Hamiltonian is an example of such a coupling, where $\hat{F} \propto \hat{n}$, the intracavity photon number.

Classically, including this force in Newton's equation yields a Langevin equation:

$$M\ddot{x} = -M\omega_M^2 x - M\gamma_{\text{cl}}\dot{x} + F_{\text{cl}}(t). \quad (3.13)$$

In addition to the noisy force, we have included a damping term (rate γ_{cl}). This will prevent the oscillator from being infinitely heated by the noise source; we can think of it as describing the average value of the force exerted on the oscillator by the noise source, which is now playing the role of a dissipative bath. If this bath is in thermal equilibrium at temperature T , we also expect the oscillator to equilibrate to the same temperature. This implies that the heating effect of $F_{\text{cl}}(t)$ must be precisely balanced by the energy-loss effect of the damping force. More explicitly, one can use Eq. (3.13) to derive an equation for the average energy of the oscillator $\langle E \rangle$. As we are assuming a weak coupling between the bath and the oscillator, we can take $\gamma_{\text{cl}} \ll \omega_M$, and hence find

$$\frac{d}{dt}\langle E \rangle = -\gamma_{\text{cl}}\langle E \rangle + \frac{\mathcal{S}_{FF}[\omega_M]}{2M}. \quad (3.14)$$

where $\mathcal{S}_{FF}[\omega]$ is the classical noise spectral density associated with $F_{\text{cl}}(t)$ (c.f. Eq. (3.9)).

Insisting that the stationary value of $\langle E \rangle$ obey equipartition then leads directly to the classical fluctuation dissipation relation:

$$\mathcal{S}_{FF}[\omega_M] = 2M\gamma_{\text{cl}}k_B T. \quad (3.15)$$

Let's now look at our problem quantum mechanically. Writing \hat{x} in terms of ladder operators, we see that \hat{H}_{int} will cause transitions between different oscillator Fock states. Treating \hat{H}_{int} in perturbation theory, we thus derive Fermi Golden rule transition rates $\Gamma_{n\pm 1, n}$ for transitions from the n to the $n \pm 1$ Fock state. As shown explicitly in Appendix B of (Clerk *et al.*, 2010), these rates can be directly tied to the quantum noise spectral density associated with \hat{F} . One finds:

$$\Gamma_{n+1, n} = (n+1) \frac{x_{\text{ZPF}}^2}{\hbar^2} \mathcal{S}_{FF}[-\omega_M] \equiv (n+1)\Gamma_{\uparrow}, \quad (3.16)$$

$$\Gamma_{n-1, n} = (n) \frac{x_{\text{ZPF}}^2}{\hbar^2} \mathcal{S}_{FF}[\omega_M] \equiv n\Gamma_{\downarrow}. \quad (3.17)$$

Transitions where the noise source absorbs energy are set by the negative frequency part of the noise spectral density, while emission is set by the positive frequency part.

We can now write a simple master equation for the probability $p_n(t)$ that the oscillator is in the n th Fock state:

$$\frac{d}{dt}p_n = [n\Gamma_{\uparrow}p_{n-1} + (n+1)\Gamma_{\downarrow}p_{n+1}] - [n\Gamma_{\downarrow} + (n+1)\Gamma_{\uparrow}]p_n. \quad (3.18)$$

We can then connect this quantum picture to our classical Langevin equation by using Eq. (3.18) to derive an equation for the average oscillator energy $\langle E \rangle$. One obtains

$$\frac{d}{dt}\langle E \rangle = -\gamma\langle E \rangle + \frac{\bar{S}_{FF}[\omega_M]}{2M}, \quad (3.19)$$

where:

$$\gamma = \frac{x_{\text{ZPF}}^2}{\hbar^2} (S_{FF}[\omega_M] - S_{FF}[-\omega_M]), \quad (3.20)$$

$$\bar{S}_{FF}[\Omega] = \frac{S_{FF}[\omega_M] + S_{FF}[-\omega_M]}{2}. \quad (3.21)$$

We see that the quantum equation for the average energy, Eq. (3.19), has an identical form to the classical equation (Eq. (3.14)), which gives us a simple way to connect our quantum noise spectral density to quantities in the classical theory:

- The symmetrized quantum noise spectral density $\bar{S}_{FF}[\Omega]$ defined in Eq. (3.21) plays the same role as the classical noise spectral density $S_{FF}[\Omega]$: it heats the oscillator the same way a classical stochastic force would.
- The asymmetric-in-frequency part of the quantum noise spectral density $S_{FF}[\Omega]$ is directly related to the damping rate γ in the classical theory. The asymmetry between absorption and emission events leads to a net energy flow between the oscillator and the noise source, analogous to what one obtains from a classical viscous damping force.

We thus see that there is a direct connection to a classical noise spectral density, and moreover the “extra information” in the asymmetry of a quantum noise spectral density also corresponds to a seemingly distinct classical quantity, a damping rate. This latter connection is not so surprising. The asymmetry of the quantum noise is a direct consequence of (here) $[\hat{F}(t), \hat{F}(t')] \neq 0$. However, this same non-commutation causes the average value of $\langle \hat{F} \rangle$ to change in response to $\hat{x}(t)$ via the interaction Hamiltonian of Eq. (3.12). Using standard quantum linear response (i.e. first-order time-dependent perturbation theory, see e.g. Ch. 6 of (Bruus and Flensberg, 2004)), one finds

$$\delta\langle \hat{F}(t) \rangle = \int_{-\infty}^{\infty} dt' \chi_{FF}(t-t')\langle \hat{x}(t') \rangle, \quad (3.22)$$

where the force-force susceptibility is given by the Kubo formula:

$$\chi_{FF}(t) \equiv \frac{-i}{\hbar}\theta(t) \left\langle \left[\hat{F}(t), \hat{F}(0) \right] \right\rangle. \quad (3.23)$$

16 Quantum limit on continuous position detection

From the classical Langevin equation Eq. (3.13), we see that part of $\langle \hat{F}(t) \rangle$ which is in phase with \dot{x} is the damping force. This leads to the definition

$$\gamma = \frac{1}{M\Omega} (-\text{Im } \chi_{FF}[\Omega]). \quad (3.24)$$

An explicit calculation shows that the above definition is identical to Eq. (3.20), which expresses γ in terms of the noise asymmetry. Note that in the language of many-body Green functions, $-\text{Im } \chi_{FF}$ is referred to as a spectral function, whereas the symmetrized noise $\bar{S}_{FF}[\omega]$ is known (up to a constant) as the ‘‘Keldysh’’ Green function.

Quantum fluctuation-dissipation theorem and notion of effective temperature. Consider the case where the quantum system producing the noise \hat{F} is in thermal equilibrium at temperature T . For weak coupling, we expect that the stationary value of $\langle E \rangle$ as given by Eq. (3.19) should match the thermal equilibrium value $\hbar\omega_M (1/2 + n_B[\omega_M])$. Insisting that this be the case forces a relation between the damping γ (which is set by the asymmetry of the noise, c.f. Eq. (3.20)) and symmetrized noise $\bar{S}_{FF}[\omega_M]$ which is nothing more than the quantum version of the fluctuation dissipation theorem:

$$\bar{S}_{FF}[\omega_M] = M\gamma[\omega_M] \hbar\omega_M \coth\left(\frac{\hbar\omega_M}{2k_B T}\right) = M\gamma[\omega_M] \hbar\omega_M (1 + 2n_B[\omega_M]). \quad (3.25)$$

For $k_B T \gg \hbar\omega_M$ this reproduces the classical result of Eq. (3.15), whereas in the opposite limit, it describes zero-point noise. We stress that Eq. (3.25) can also be proved directly using nothing more than the fact that the system producing the noise has a thermal-equilibrium density matrix.

What happens if our noise source is *not* in thermal equilibrium? In that case, it is useful to use Eq. (3.25) to *define* an effective temperature $T_{\text{eff}}[\Omega]$ from the ratio of the symmetrized noise and damping. Re-writing things in terms of the quantum noise spectral density, one finds

$$k_B T_{\text{eff}}[\Omega] \equiv \hbar\Omega \left[\ln \left(\frac{S_{FF}[\Omega]}{S_{FF}[-\Omega]} \right) \right]^{-1}. \quad (3.26)$$

The effective temperature at a given frequency Ω characterizes the asymmetry between absorption and emission rates of energy $\hbar\Omega$; a large temperature indicates that these rates are almost equal, whereas a small temperature indicates that emission by the noise source is greatly suppressed compared to absorption by the source. Away from thermal equilibrium, there is no guarantee that the ratio on the RHS will be frequency-independent, and hence T_{eff} will generally have a frequency dependence.

3.3 Heisenberg inequality on detector quantum noise

3.3.1 Generic two-port linear response detector

Having discussed two of the ways quantum noise spectral densities differ from their classical counterparts (zero-point noise, frequency asymmetry), we now turn to the third distinguishing feature: there are purely quantum constraints on the noise properties of any system capable of acting as a detector or amplifier. We will be interested

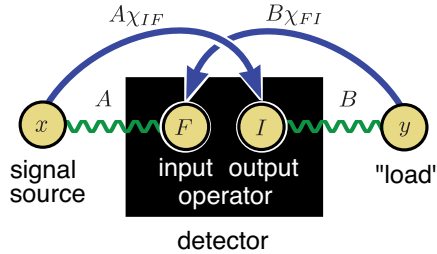


Fig. 3.1 (Color online) Schematic of a generic linear response detector.

in the generic two-port detector sketched in Fig. 3.1. The detector has an input port characterized by an operator \hat{F} : this is the detector quantity which couples to the system we wish to measure. Similarly, the output port is characterized by an operator \hat{I} : this is the detector quantity that we will readout to learn about the system coupled to the input. In our optomechanical system, \hat{F} would be the cavity photon number \hat{n} , while \hat{I} would be proportional to the phase quadrature of the output field of the cavity (c.f. Eq. (3.3)).

We will be interested almost exclusively in detector-signal couplings weak enough that one can use linear-response to describe how \hat{I} changes in response to the signal. For example, if we couple an input signal \hat{x} to our detector via an interaction Hamiltonian

$$\hat{H}_{\text{int}} = \hat{x} \cdot \hat{F}, \quad (3.27)$$

linear response tells us that the change in the detector output will be given by:

$$\delta \langle \hat{I}(t) \rangle = \int_{-\infty}^{\infty} dt' \chi_{IF}(t-t') \langle \hat{x}(t') \rangle, \quad (3.28)$$

$$\chi_{IF}(t) = -\frac{i}{\hbar} \theta(t) \langle [\hat{I}(t), \hat{F}(0)] \rangle. \quad (3.29)$$

This is completely analogous to the way we discussed damping, c.f. Eq. (3.24). As is standard in linear-response, the expectation value in Eq. (3.29) is with respect to the state of the system (signal plus detector) at zero coupling (i.e. $\hat{H}_{\text{int}} = 0$). Also, without loss of generality, we will assume that both $\langle \hat{I} \rangle$ and $\langle \hat{F} \rangle$ are zero in the absence of any coupling to the input signal.

Even on a classical level, any noise in the input and output ports will limit our ability to make measurements with the detector. Quantum mechanically, we have seen that it is the symmetrized quantum spectral densities that play a role analogous to classical noise spectral densities. We will thus be interested in the quantities $\tilde{S}_{II}[\omega]$ and $\tilde{S}_{FF}[\omega]$. Given our interest in weak detector-signal couplings, it will be sufficient to characterize the detector noise at zero-coupling to the detector.

In addition to \tilde{S}_{II} , \tilde{S}_{FF} , we will also have to contend with the fact that the noise in \hat{I} and \hat{F} may be correlated. Classically, we would describe such correlations via a correlation spectral density $\mathcal{S}_{IF}[\omega]$:

18 Quantum limit on continuous position detection

$$\mathcal{S}_{IF}[\omega] \equiv \lim_{T \rightarrow \infty} \langle I_T[\omega] (F_T[\omega])^* \rangle = \int_{-\infty}^{\infty} dt \langle I(t) F(0) \rangle e^{i\omega t}, \quad (3.30)$$

where the Fourier transforms $I_T[\omega]$ and $F_T[\omega]$ are defined analogously to Eq. (3.8). Not surprisingly, such classical correlations correspond to a symmetrized quantum noise spectral density

$$\bar{\mathcal{S}}_{IF}[\omega] \equiv \frac{1}{2} \int_{-\infty}^{\infty} dt \langle \{\hat{I}(t), \hat{F}(0)\} \rangle e^{i\omega t}. \quad (3.31)$$

Note that the classical correlation density $\mathcal{S}_{IF}[\omega]$ is generally complex, and is only guaranteed to be real at $\omega = 0$; the same is true of $\bar{\mathcal{S}}_{IF}[\omega]$.

Finally, we normally are only concerned about how large the output noise is compared to the magnitude of the “amplified” input signal at the output (i.e. Eq. (3.28)). It is thus common to think of the output noise at a given frequency $\delta I_T[\omega]$ as an equivalent fluctuation of the signal $\delta z_{\text{imp}}[\omega] \equiv \delta I_T[\omega] / \chi_{IF}[\omega]$. We thus define the imprecision noise spectral density and imprecision-back-action correlation density as:

$$\bar{\mathcal{S}}_{zz}[\omega] \equiv \frac{\bar{\mathcal{S}}_{II}[\omega]}{|\chi_{IF}[\omega]|^2}, \quad \bar{\mathcal{S}}_{zF}[\omega] \equiv \frac{\bar{\mathcal{S}}_{IF}[\omega]}{\chi_{IF}[\omega]}. \quad (3.32)$$

3.3.2 Motivation and derivation of noise constraint

We can now ask what sort of constraints exist on the detector noise. In almost all relevant cases, our detector will be some sort of driven quantum system, and hence will not be in thermal equilibrium. As a result, any meaningful constraint should not rely on having a thermal equilibrium state. Classically, all we can say is that the correlations in the noise cannot be bigger than the noise itself. This constraint takes the form of a Schwartz inequality, yielding

$$\mathcal{S}_{zz}[\omega] \mathcal{S}_{FF}[\omega] \geq |\mathcal{S}_{zF}[\omega]|^2. \quad (3.33)$$

Equality here implies a perfect correlation, i.e. $I_T[\omega] \propto F_T[\omega]$.

Quantum mechanically, additional constraints will emerge. Heuristically, this can be expected by making an analogy to the example of the Heisenberg microscope. In that example, one finds that there is a tradeoff between the imprecision of the measurement (i.e. the position resolution) and the back-action of the measurement (i.e. the momentum kick delivered to the particle). In our detector, noise in \hat{I} will correspond to the imprecision of the measurement (i.e. the bigger this noise, the harder it will be to resolve the signal described by Eq. (3.28)). Similarly, noise in \hat{F} is the back-action: as we already saw, by virtue of the detector-signal coupling, \hat{F} acts as a noisy force on the measured quantity \hat{z} . We thus might naturally expect a bound on the product of $\bar{\mathcal{S}}_{zz} \bar{\mathcal{S}}_{FF}$.

Alternatively, we see from Eq. (3.29) that for our detector to have any response at all, $\hat{I}(t)$ and $\hat{F}(t')$ cannot commute for all times. Quantum mechanically, we know that uncertainty relations apply any time we have non-commuting observables; here things are somewhat different, as the non-commutation is between Heisenberg-picture operators at different times. Nonetheless, we can still use the standard derivation of an

uncertainty relation to obtain a useful constraint. Recall that for two non-commuting observables \hat{A} and \hat{B} , the full Heisenberg inequality is (see, e.g. (Gottfried, 1966))

$$(\Delta A)^2(\Delta B)^2 \geq \frac{1}{4} \left\langle \{ \hat{A}, \hat{B} \} \right\rangle^2 + \frac{1}{4} \left| \left\langle [\hat{A}, \hat{B}] \right\rangle \right|^2. \quad (3.34)$$

Here we have assumed $\langle \hat{A} \rangle = \langle \hat{B} \rangle = 0$. We now take \hat{A} and \hat{B} to be cosine-transforms of \hat{I} and \hat{F} , respectively, over a finite time-interval T :

$$\hat{A} \equiv \sqrt{\frac{2}{T}} \int_{-T/2}^{T/2} dt \cos(\omega t + \delta) \hat{I}(t), \quad \hat{B} \equiv \sqrt{\frac{2}{T}} \int_{-T/2}^{T/2} dt \cos(\omega t) \hat{F}(t). \quad (3.35)$$

Note that we have phase shifted the transform of \hat{I} relative to that of \hat{F} by a phase δ . In the limit $T \rightarrow \infty$ we find

$$\bar{S}_{zz}[\omega] \bar{S}_{FF}[\omega] \geq [\text{Re} (e^{i\delta} \bar{S}_{zF}[\omega])]^2 + \frac{\hbar^2}{4} \left[\text{Re} e^{i\delta} \left(1 - \frac{(\chi_{FI}[\omega])^*}{\chi_{IF}[\omega]} \right) \right]^2. \quad (3.36)$$

We have introduced here a new susceptibility $\chi_{FI}[\omega]$, which describes the reverse response coefficient or reverse gain of our detector. This is the response coefficient relevant if we used our detector in reverse: couple the input signal \hat{z} to \hat{I} , and see how $\langle \hat{F} \rangle$ changes. A linear response relation analogous to Eq. (3.28) would then apply, with $F \leftrightarrow I$ everywhere. For the optomechanical system we are most interested in, this reverse response coefficient vanishes: coupling to the output field from the cavity cannot change the intracavity photon number (and hence \hat{F}). We thus take $\chi_{FI}[\omega] = 0$ in what follows (see (Clerk, Devoret, Girvin, Marquardt and Schoelkopf, 2010) for further discussion on the role of a non-zero $\chi_{FI}[\omega]$).

If we now maximize the RHS of Eq. (3.36) over all values of δ , we are left with the optimal bound

$$\bar{S}_{zz}[\omega] \bar{S}_{FF}[\omega] - |\bar{S}_{zF}[\omega]|^2 \geq \frac{\hbar^2}{4} \left(1 + \Delta \left[\frac{2\bar{S}_{zF}[\omega]}{\hbar} \right] \right), \quad (3.37)$$

where

$$\Delta[y] = \frac{|1 + y^2| - (1 + |y|^2)}{2}, \quad (3.38)$$

Note that for any complex number y , $1 + \Delta[y] > 0$. Related noise constraints on linear-response detectors are presented in (Braginsky and Khalili, 1996) and (Averin, 2003).

We see that applying the uncertainty principle to our detector has given us a rigorous constraint on the detector's noise which is stronger than the simple classical bound of Eq. (3.33) on its correlations. For simplicity, consider first the $\omega \rightarrow 0$ limit, where all noise spectral densities and susceptibilities are real, and hence the term involving $\Delta[y]$ vanishes. The extra quantum term on the RHS of Eq. (3.36) then implies:

20 Quantum limit on continuous position detection

- The product of the imprecision noise \bar{S}_{zz} and back-action noise \bar{S}_{FF} cannot be zero. The magnitude of both kinds of fluctuations must be non-zero.
- Moreover, these fluctuations cannot be perfectly correlated with one another: we cannot have $(\bar{S}_{zF})^2 = \bar{S}_{zz}\bar{S}_{FF}$.

The presence of these extra quantum constraints on noise will lead directly (and rigorously!) to the fundamental quantum limits on continuous position detection. As we will see, reaching this quantum limit requires one to use a detector which has “ideal” quantum noise (i.e. noise spectral densities for which the inequality of Eq. (3.37) becomes an equality).

3.4 Power gain and the large gain limit

Before finally turning to defining and deriving the quantum limit on the added noise, there is one more crucial aspect of the detector to address: the notion of “power gain”. We are interested in detectors that turn the motion $x(t)$ of the mechanical resonator into a “large” signal in the output of the detector, a signal so large that we do not need to worry about how this detector output is then read out. To be able to say that our detector truly amplifies the motion of the oscillator, it is not sufficient to simply say the response function χ_{IF} must be large (note that χ_{IF} is not dimensionless!). Instead, true amplification requires that the *power* delivered by the detector to a following amplifier be much larger than the power drawn by the detector at its input—i.e., the detector must have a dimensionless power gain $G_P[\omega]$ much larger than one. If the power gain was not large, we would need to worry about the next stage in the amplification of our signal, and how much noise is added in that process. Having a large power gain means that by the time our signal reaches the following amplifier, it is so large that the added noise of this following amplifier is unimportant.

The power gain of our position detector can be defined by imagining a situation where one couples a second auxiliary oscillator to the output of the detector, such that $I(t)$ acts as a driving force on this oscillator. The power gain is then defined as the power delivered to this auxiliary oscillator, divided by the power drawn from the measured mechanical resonator coupled to the detector output (optimized over properties of the auxiliary oscillator). The calculation is presented in Appendix A, and the result is the simple expression:

$$G_P[\omega] \equiv \max \left[\frac{P_{\text{out}}}{P_{\text{in}}} \right] = \frac{|\chi_{IF}[\omega]|^2}{4 (\text{Im } \chi_{FF}[\omega]) (\text{Im } \chi_{II}[\omega])} \quad (3.39)$$

The susceptibility $\chi_{II}[\omega]$ is defined analogously to Eq. (3.23). Note that if there is no additional back-action damping of the measured oscillator by the detector, then $\text{Im } \chi_{FF}$ vanishes, and the power gain is strictly infinite. As we will see, this the case for an optomechanical cavity driven on resonance.

Having a large power gain also implies that we can treat the detector quantities $\hat{I}(t)$ and $\hat{F}(t)$ as being effectively “classical”. A large power gain over some relevant frequency range implies that the imaginary parts of χ_{II} and χ_{FF} are negligible over this range. From Eqs. (3.20) and (3.24), this implies that the quantum noise spectral densities $S_{II}[\omega]$, $S_{FF}[\omega]$ are to a good approximation *symmetric* over these frequencies,

just like a classical noise spectral density. This in turn implies that one can effectively treat $[\hat{I}(t), \hat{I}(t')] = [\hat{F}(t), \hat{F}(t')] = 0$ (i.e. these operators commute at different times, just like a classical noisy function of time). We note that in many discussions of linear quantum measurements, the fact that the detector input and output quantities commute with themselves at different times is taken as a starting assumption in calculations (see, e.g. (Braginsky and Khalili, 1992; Khalili *et al.*, 2012), as well as the lectures by Y. Chen).

Requiring both the quantum noise inequality in Eq. (3.37) to be saturated at frequency ω as well as a large power gain (i.e. $G_P[\omega] \gg 1$) leads to some important additional constraints on the detector, as derived in Appendix I of (Clerk *et al.*, 2010):

- $(2/\hbar)\text{Im} \bar{S}_{zF}[\omega]$ is small like $1/\sqrt{G_P[\omega]}$.
- The detector's effective temperature must be much larger than $\hbar\omega$; one finds

$$k_B T_{\text{eff}}[\omega] \sim \sqrt{G_P[\omega]} \hbar\omega. \quad (3.40)$$

Conversely, it is the largeness of the detector's effective temperature that allows it to have a large power gain.

3.5 Defining the quantum limit

Having now understood the proper way to discuss the “size” of noise, as well as the existence of quantum constraints on noise, we can now return to the question posed at the start of this chapter: how small can we make the added noise $\delta x_{\text{add}}(t)$ (c.f. Eq. (3.6)) of a generic linear-response position detector? We assume that, like in our optomechanical setup, the detector couples to mechanical position via a Hamiltonian:

$$\hat{H}_{\text{int}} = \hat{x} \cdot (A\hat{F}) \quad (3.41)$$

Note that unlike the generic system-detector interaction in Eq.(3.27), we have included a coupling strength in the definition of the system operator \hat{F} . We assume that A is weak enough that the detector output responds linearly to changes in position.

3.5.1 Added noise spectral density

We start by returning to the heuristic classical expression in Eq. (3.6) for the detector output current $I(t)$ and added noise $\delta x_{\text{add}}(t)$, and Fourier transform these expression. From linear response theory, we know that the response coefficient λ in that expression should be replaced by $\lambda \rightarrow A\chi_{IF}[\omega]$, where the frequency dependence parameterizes that the detector output will not respond instantaneously to changes at the input.

$$I[\omega] = A\chi_{IF}[\omega] (x[\omega] + \delta x_{\text{add}}[\omega]) \quad (3.42)$$

$$\delta x_{\text{add}}[\omega] = \delta x_{\text{BA}}[\omega] + \frac{\delta I_0[\omega]}{A\chi_{IF}[\omega]} \quad (3.43)$$

The first back-action term is just the mechanical response to the back-action force fluctuations:

22 Quantum limit on continuous position detection

$$\delta x_{\text{BA}}[\omega] = A\chi_{xx}[\omega]\delta F[\omega], \quad (3.44)$$

where $\chi_{xx}[\omega]$ is the oscillator's force susceptibility¹, and is given by

$$M\chi_{xx}[\omega] = (\omega^2 - \omega_M^2 + i\omega\gamma_0)^{-1}. \quad (3.45)$$

To state the quantum limit on position detection, we first define the total measured position fluctuations $x_{\text{meas}}[\omega]$ as simply the total detector output $I[\omega]$ referred back to the oscillator:

$$x_{\text{meas}}[\omega] = I_{\text{tot}}[\omega]/(A\chi_{IF}[\omega]). \quad (3.46)$$

If there was *no* added noise, and further, if the oscillator was in thermal equilibrium at temperature T , the spectral density describing the fluctuations $\delta x_{\text{meas}}(t)$ would simply be the equilibrium fluctuations of the oscillator, as given by the fluctuation-dissipation theorem:

$$\bar{S}_{xx}^{\text{meas}}[\omega] = \bar{S}_{xx}^{\text{eq}}[\omega, T] = \hbar \coth\left(\frac{\hbar\omega}{2k_B T}\right) [-\text{Im} \chi_{xx}[\omega]] \quad (3.47)$$

$$= \frac{x_{\text{ZPF}}^2(1 + 2n_B)}{2} \sum_{\sigma=\pm} \frac{\gamma_0}{(\omega - \sigma\Omega)^2 + (\gamma_0/2)^2}. \quad (3.48)$$

Here, γ_0 is the intrinsic damping rate of the oscillator, which we have assumed to be $\ll \Omega$.

Including the added noise, and for the moment ignoring the possibility of any additional oscillator damping due to the coupling to the detector, the above result becomes

$$\bar{S}_{xx}^{\text{meas}}[\omega] = \bar{S}_{xx}^{\text{eq}}[\omega, T] + \bar{S}_{xx}^{\text{add}}[\omega] \quad (3.49)$$

where the last term is the spectral density of the added noise (both back-action and imprecision noise).

We can now, finally, state the quantum limit on continuous position detection: at each frequency ω , we must have

$$\bar{S}_{xx}^{\text{add}}[\omega] \geq \bar{S}_{xx}^{\text{eq}}[\omega, T = 0]. \quad (3.50)$$

The spectral density of the added noise cannot be made arbitrarily small: at each frequency, it must be at least as large as the corresponding zero-point noise. Note that we do not call this the ‘‘standard’’ quantum limit. As we will discuss later, what is usually termed the standard quantum limit (e.g. in the gravitational wave detection community) only coincides with Eq. (3.50) exactly at resonance ($\omega = \omega_M$), and for other frequencies does not represent any kind of true quantum bound. The various contributions to the added noise spectral density are shown in Fig. 3.2.

Finally, the above result can be refined to include situations where the coupling to the detector also changes the mechanical damping (in addition to driving it with extra

¹Strictly speaking, with our definitions the force susceptibility is $-\chi_{xx}[\omega]$, and the force driving the mechanics is $-\hat{F}$. This is because we took the interaction Hamiltonian to be $\hat{H}_{\text{int}} = +\hat{x}\hat{F}$ instead of the more physical $\hat{H}_{\text{int}} = -\hat{x}\hat{F}$.

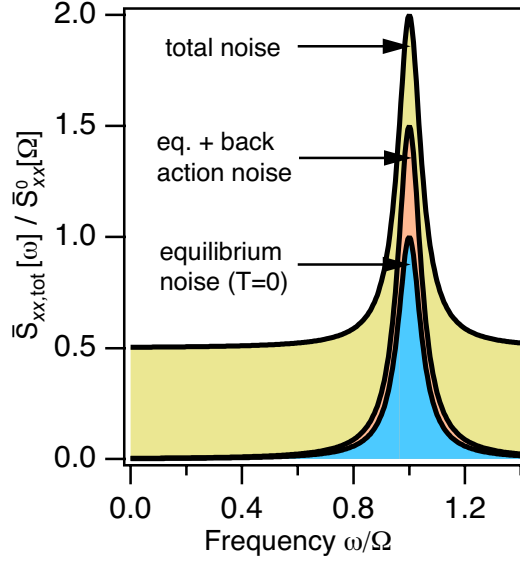


Fig. 3.2 Spectral density of a mechanical resonator’s position fluctuations as measured by a quantum limited position detector. The mechanical resonator’s intrinsic fluctuations (for the case of a zero-temperature oscillator) are shown in blue. The back-action of the position detector will effectively heat the mechanical resonator, increasing the area under the Lorentzian; this is shown as the orange area. Finally, there is also imprecision noise, the fluctuations in the detector output that would be present even without any coupling to the mechanical resonator. These typically give frequency independent noise, giving a flat background. The ideal case where the quantum-limit is reached on the added noise at mechanical resonance is the yellow area.

fluctuations). Letting γ_{BA} denote this extra damping, the added noise is now defined via

$$\bar{S}_{xx}^{\text{meas}}[\omega] = \frac{\gamma_0}{\gamma_{\text{BA}} + \gamma_0} \bar{S}_{xx}^{\text{eq}}[\omega, T] + \bar{S}_{xx}^{\text{add}}[\omega], \quad (3.51)$$

where the susceptibility χ_{xx} now involves the total damping of the oscillator, i.e.:

$$M\chi_{xx}[\omega] = (\omega^2 - \omega_M^2 + i\omega(\gamma + \gamma_{\text{BA}}))^{-1}. \quad (3.52)$$

With this definition, the quantum limit on the added noise is unchanged from the limit stated in Eq. (3.50).

3.5.2 A possible correlation-based loophole?

Our heuristic formulation of the quantum limit naturally leads to a possible concern. Even though quantum mechanics may require a position measurement to have a back-action (as position and momentum are conjugate quantities), couldn’t this back-action

24 Quantum limit on continuous position detection

noise be perfectly anti-correlated with the imprecision noise? If this were the case, the added noise $\delta x(t)$ (which is the sum of the two contributions, c.f. Eq. (3.43)) could be made to vanish.

One might hope that this sort of loophole would be explicitly forbidden by the quantum noise inequality of Eq. (3.37). However, this is not the case. Even in the ideal case of zero reverse gain, one can achieve a situation where back-action and imprecision are perfectly correlated at a given non-zero frequency ω . One needs:

- The correlator $\bar{S}_{IF}[\omega]$ should be purely imaginary; this implies that the part of $F(t)$ that is correlated with $I(t)$ is 90 degrees out of phase. Note that $\bar{S}_{IF}[\omega]$ can only be imaginary at non-zero frequencies.
- The magnitude of $\bar{S}_{IF}[\omega]$ should be larger than $\hbar/2$

Under these circumstances, one can verify that there is no additional quantum constraint on the noise beyond what exists classically, and hence the perfect correlation condition of $\bar{S}_{FF}[\omega]\bar{S}_{II}[\omega] = |\bar{S}_{IF}[\omega]|^2$ is allowable. The $\pi/2$ phase of the back-action-imprecision correlations are precisely what is needed to make $\delta x_{\text{add}}[\omega]$ vanish at the oscillator resonance, $\omega = \Omega$.

As might be expected, this seeming loophole is *not* a route to ideal, noise-free position detection free from quantum constraints. As already discussed, we need to be more careful in specifying what we want our detector to do. We aren't interested in just having the mechanical motion show up in the detector output $I(t)$, we want there to be amplification associated with this process—the mechanical signal should be “bigger” at the output than it is at the input. It is only when we insist on amplification that there are quantum constraints on added noise; a passive transducer need not add any noise. On a heuristic level, one could view amplification as an effective expansion of the phase space of the oscillator. Such a pure expansion is of course forbidden by Liouville's theorem, which tells us that volume in phase space is conserved. The way out is to introduce additional degrees of freedom, such that for these degrees of freedom phase space contracts. Quantum mechanically such degrees of freedom necessarily have noise associated with them (at the very least, zero-point noise); this then is the source of the limit on added noise.

The requirement that our detector produces a large signal is that the power gain (as defined in Sec. 3.4) should be much larger than one. In that case, back-action-imprecision correlations must be purely real, and the possibility of zero added noise (due to perfect correlations) is excluded.

3.6 Derivation of the quantum limit

We now turn to a rigorous proof of the quantum limit on the added noise given in Eq. (3.50). From the classical-looking Eq. (3.43), we expect that the symmetrized quantum noise spectral density describing the added noise will be given by

$$\bar{S}_{xx,\text{add}}[\omega] = \frac{\bar{S}_{II}}{|\chi_{IF}|^2 A^2} + A^2 |\chi_{xx}|^2 \bar{S}_{FF} + \frac{2\text{Re} [\chi_{IF}^* (\chi_{xx})^* \bar{S}_{IF}]}{|\chi_{IF}|^2} \quad (3.53)$$

$$= \frac{\bar{S}_{zz}}{A^2} + A^2 |\chi_{xx}|^2 \bar{S}_{FF} + 2\text{Re} [(\chi_{xx})^* \bar{S}_{zF}]. \quad (3.54)$$

In the second line, we have introduced the imprecision noise \bar{S}_{zz} and imprecision back-action correlation \bar{S}_{zF} as in Eq. (3.32). We have also omitted writing the explicit frequency dependence of the gain χ_{IF} , susceptibility χ_{xx} , and noise correlators; they should all be evaluated at the frequency ω . Finally, the oscillator susceptibility χ_{xx} here is given by Eq. (3.52), and includes the effects of back-action damping. While we have motivated this equation from a seemingly classical noise description, the full quantum theory also yields the same result: one simply calculates the detector output noise perturbatively in the coupling to the oscillator (Clerk, 2004).

The first step in determining the limit on the added noise is to consider its dependence on the coupling strength A . If we ignore for a moment the detector-dependent damping of the oscillator, there will be an optimal value of the coupling strength A which corresponds to a trade-off between imprecision noise and back-action (i.e. first and second terms in Eq. (3.53)). We would thus expect $\bar{S}_{xx,\text{add}}[\omega]$ to attain a minimum value at an optimal choice of coupling $A = A_{\text{opt}}$ where both these terms make equal contributions. Defining $\phi[\omega] = \arg \chi_{xx}[\omega]$, we thus have the bound

$$\bar{S}_{xx,\text{add}}[\omega] \geq 2|\chi_{xx}[\omega]| \left(\sqrt{\bar{S}_{zz}\bar{S}_{FF}} + \text{Re} \left[e^{-i\phi[\omega]} \bar{S}_{zF} \right] \right), \quad (3.55)$$

where the minimum value at frequency ω is achieved when

$$A_{\text{opt}}^2 = \sqrt{\frac{\bar{S}_{zz}[\omega]}{|\chi_{xx}[\omega]|^2 \bar{S}_{FF}[\omega]}}. \quad (3.56)$$

Using the inequality $X^2 + Y^2 \geq 2|XY|$ we see that this value serves as a lower bound on $\bar{S}_{xx,\text{add}}$ even in the presence of detector-dependent damping. In the case where the detector-dependent damping is negligible, the RHS of Eq. (3.55) is independent of A , and thus Eq. (3.56) can be satisfied by simply tuning the coupling strength A ; in the more general case where there is detector-dependent damping, the RHS is also a function of A (through the response function $\chi_{xx}[\omega]$), and it may no longer be possible to achieve Eq. (3.56) by simply tuning A .

While Eq. (3.55) is certainly a bound on the added displacement noise $\bar{S}_{xx,\text{add}}[\omega]$, it does not in itself represent the quantum limit. Reaching the quantum limit requires more than simply balancing the detector back-action and intrinsic output noises (i.e. the first two terms in Eq. (3.53)); *one also needs a detector with “quantum-ideal” noise properties, that is a detector which optimizes Eq. (3.37)*. Using the quantum noise constraint of Eq. (3.37) to further bound $\bar{S}_{xx,\text{add}}[\omega]$, we obtain

$$\bar{S}_{xx,\text{add}}[\omega] \geq \hbar |\chi_{xx}[\omega]| \left[\sqrt{\left(1 + \Delta \left[\frac{\bar{S}_{zF}}{\hbar/2} \right] \right)^2 + \left| \frac{\bar{S}_{zF}}{\hbar/2} \right|^2} + \frac{\text{Re} \left[e^{-i\phi[\omega]} \bar{S}_{zF} \right]}{\hbar/2} \right], \quad (3.57)$$

where the function $\Delta[z]$ is defined in Eq. (3.38). The minimum value of $\bar{S}_{xx,\text{add}}[\omega]$ in Eq. (3.57) is now achieved when one has *both* an optimal coupling (i.e. Eq. (3.56)) and a quantum limited detector, that is one which satisfies Eq. (3.37) as an equality.

Next, we further specialize to the relevant case where the detector acts as a good amplifier, and has a power gain $G_P[\omega] \gg 1$ over all frequencies of interest. As discussed, this implies that the ratio \bar{S}_{zF} is purely real up to small $1/G_P$ corrections (see

Appendix I of Ref. (Clerk *et al.*, 2010) for more details). This in turn implies that $\Delta[2\bar{S}_{zF}/\hbar] = 0$; we thus have

$$\bar{S}_{xx,\text{add}}[\omega] \geq \hbar|\chi_{xx}[\omega]| \left[\sqrt{1 + \left(\frac{\bar{S}_{zF}}{\hbar/2}\right)^2} + \cos(\phi[\omega]) \frac{\bar{S}_{zF}}{\hbar/2} \right]. \quad (3.58)$$

Finally, as there is no further constraint on \bar{S}_{zF} (beyond the fact that it is real), we can minimize the expression over its value. The minimum $\bar{S}_{xx,\text{add}}[\omega]$ is achieved for a detector whose cross-correlator satisfies

$$\bar{S}_{zF}[\omega] \Big|_{\text{optimal}} = \frac{\hbar}{2} \cot \phi[\omega] = -\frac{\hbar}{2} \frac{\omega^2 - \omega_M^2}{\omega\gamma}, \quad (3.59)$$

with the minimum value of the added noise being given precisely by

$$\bar{S}_{xx,\text{add}}[\omega] \Big|_{\text{min}} = \hbar|\text{Im } \chi_{xx}[\omega]| = \lim_{T \rightarrow 0} \bar{S}_{xx,\text{eq}}[\omega, T], \quad (3.60)$$

in agreement with Eq. (3.50). Thus, in the limit of a large power gain, we have that *at each frequency, the minimum displacement noise added by the detector is precisely equal to the noise arising from a zero temperature bath.*

3.7 Simple limits and discussion

We have thus provided a rigorous derivation of the quantum limit on the added noise of a continuous position detector which possesses a large gain. The derivation shows explicitly what is needed to reach the quantum-limit, namely:

1. A detector with quantum limited noise properties, that is one which optimizes the inequality of Eq. (3.37).
2. A coupling A which satisfies Eq. (3.56).
3. A detector cross-correlator \bar{S}_{IF} which satisfies Eq. (3.59).

It is worth stressing that Eq. (3.59) implies that it will *not* in general be possible to achieve the quantum limit simultaneously at all frequencies, as the needed amount of back-action-imprecision correlation varies strongly with frequency. We consider a few important limits below.

3.7.1 Quantum limit on added noise at resonance $\omega = \omega_M$

To reach the quantum limit on the added noise at the mechanical resonance, Eq. (3.59) tells us that $\bar{S}_{zF}[\omega]$ must be zero: back-action and imprecision noises should be completely uncorrelated. If this is the case, reaching the quantum limit simply involves tuning the coupling A to balance the contributions from back-action and imprecision to the added noise. As we will see, in our optomechanical cavity, this is equivalent to optimizing the choice of the driving power.

This remaining condition on the coupling (again, in the limit of a large power gain) may be written as

$$\frac{\gamma_{\text{BA}}[A_{\text{opt}}]}{\gamma_0 + \gamma_{\text{BA}}[A_{\text{opt}}]} = \frac{\hbar\Omega}{4k_{\text{B}}T_{\text{eff}}}. \quad (3.61)$$

As $\gamma_{\text{BA}}[A] \propto A^2$ is the back-action-induced damping of the oscillator (c.f. Eq. (3.20)), we thus have that *to achieve the quantum-limited value of $\bar{S}_{xx,\text{add}}[\Omega]$ with a large power gain, one needs the intrinsic damping of the oscillator to be much larger than the back-action damping*. The back-action damping must be small enough to compensate the large effective temperature of the detector; if the bath temperature satisfies $\hbar\Omega/k_{\text{B}} \ll T_{\text{bath}} \ll T_{\text{eff}}$, Eq. (3.61) implies that at the quantum limit, the temperature of the oscillator will be given by

$$T_{\text{osc}} \equiv \frac{\gamma_{\text{BA}} \cdot T_{\text{eff}} + \gamma_0 \cdot T_{\text{bath}}}{\gamma_{\text{BA}} + \gamma_0} \rightarrow \frac{\hbar\Omega}{4k_{\text{B}}} + T_{\text{bath}}. \quad (3.62)$$

Thus, at the quantum limit and for large T_{eff} , the detector raises the oscillator's temperature by $\hbar\Omega/4k_{\text{B}}$.² As expected, this additional heating is only *half* the zero-point energy; in contrast, the quantum-limited value of $\bar{S}_{xx,\text{add}}[\omega]$ corresponds to the full zero-point result, as it also includes the contribution of the intrinsic output noise of the detector.

3.7.2 Quantum limit on added noise in the free-mass limit $\omega \gg \omega_{\text{M}}$

In gravitational wave detection, one is usually interested in the added noise at frequencies far above resonance, where the mechanical dynamics are effectively like those of a free mass. In this case, Eq. (3.59) tells us that reaching the quantum limit on the added noise requires back-action imprecision correlations satisfying:

$$\bar{S}_{zF}[\omega] \Big|_{\text{optimal}} \rightarrow -\frac{\hbar\omega}{2\gamma} \quad (3.63)$$

In the limit where $\omega \gg \gamma$, the correlations are huge, implying that the optimal situation is to have back-action and imprecision noises be almost perfectly correlated. If one could achieve this, the quantum limited value of the added noise is given by:

$$\bar{S}_{xx,\text{add}}[\omega] \rightarrow \frac{\hbar\gamma}{m\omega^3} \quad (3.64)$$

In contrast to the full quantum limit above, one often discusses the “standard quantum limit” in the gravitational wave detection community. This is the minimum added noise possible (in the free mass limit) if you use a detector with quantum-ideal noise (i.e. saturates the inequality of Eq. (3.37)) but which has $\bar{S}_{zF}[\omega] = 0$. In this

²If in contrast our oscillator was initially at zero temperature (i.e. $T_{\text{bath}} = 0$), one finds that the effect of the back-action (at the quantum limit and for $G_P \gg 1$) is to heat the oscillator to a temperature $\hbar\Omega/(k_{\text{B}} \ln 5) \simeq 0.62\hbar\Omega/k_{\text{B}}$.

case, the only optimization involves tuning the coupling to balance back-action and imprecision noises, and one finds:

$$\bar{S}_{xx,\text{add}}[\omega] \Big|_{\text{SQL}} = \hbar |\chi_{xx}[\omega]| \rightarrow \frac{\hbar}{m\omega^2} \quad (3.65)$$

One sees that this is larger than the true quantum limit by a large factor ω/γ .

The take-home message here is that while reaching the true quantum limit for $\omega \gg \omega_M$ might be challenging, one can do much better than the “standard” quantum limit by using a detector having back-action-imprecision correlations. In the next chapter, we will review how injecting squeezed light into an optomechanical cavity can achieve this goal.

3.8 Applications to an optomechanical cavity (with and without input squeezing)

We now apply our general approach for formulating the quantum limit to the specific case of an optomechanical cavity detector, as introduced in the first chapter. We consider a cavity which is strongly driven on resonance (implying that the detuning $\Delta = 0$), and which can be treated using the linearized equations of motion introduced in chapter 1. Our starting point is thus Eq. (2.25) for the displaced cavity field, with $\Delta = 0$. We will further work in the regime where the mechanical frequency $\omega_M \ll \kappa$, and we are interested in $\hat{d}[\omega]$ at frequencies $\omega \ll \kappa$. To capture the behaviour at these frequencies, we can make the adiabatic approximation, and ignore the $(d/dt)\hat{d}$ term on the LHS of Eq. (2.25). Defining $A = G/x_{\text{ZPF}} = g\bar{a}/x_{\text{ZPF}}$, we have:

$$\hat{d}(t) \simeq -\frac{2iA}{\kappa}\hat{x}(t) - \frac{2}{\sqrt{\kappa}}\hat{d}_{\text{in}}(t) \quad (3.66)$$

where the effective coupling strength A is given by:

$$A = \frac{G}{x_{\text{ZPF}}} = \frac{g\bar{a}_{\text{cl}}}{x_{\text{ZPF}}} \quad (3.67)$$

We see that, as anticipated, the effective coupling strength is indeed dependent on the strength of the cavity driving field. Using the input-output relation of Eq. (2.15), we also find:

$$\hat{d}_{\text{out}}(t) = \hat{d}_{\text{in}}(t) + \sqrt{\kappa}\hat{d}(t) \simeq -\frac{2iA}{\sqrt{\kappa}}\hat{x}(t) - \hat{d}_{\text{in}}(t) \quad (3.68)$$

We can use these results to calculate the needed noise properties: the fluctuations in the back-action force acting on the mechanics, and the fluctuations in the detector output quantity, the phase quadrature of the output light defined in Eq. (3.3). The back-action force operator corresponds to the fluctuating part of the intra-cavity photon number. Keeping only the drive-enhanced term in this operator, we have that:

$$A \cdot \hat{F} \equiv \hbar A \left(\hat{d} + \hat{d}^\dagger \right) \quad (3.69)$$

We need to understand the fluctuations of \hat{F} in the absence of any optomechanical coupling; we can thus substitute in Eq. (3.66) at $A = 0$ to find:

$$\hat{F} = -\frac{2\hbar}{\sqrt{\kappa}} \left(\hat{d}_{\text{in}}(t) + \hat{d}_{\text{in}}^\dagger(t) \right) \quad (3.70)$$

Similarly, the output quantity is given by the phase quadrature of the cavity output field, Eq. (3.3)³:

$$\hat{I} = i \left(d_{\text{out}} - \hat{d}_{\text{out}}^\dagger \right) \quad (3.71)$$

$$= \frac{4A}{\sqrt{\kappa}} \hat{x}(t) - i \left(\hat{d}_{\text{in}} - \hat{d}_{\text{in}}^\dagger \right) \equiv A\chi_{IF}\hat{x}(t) + \hat{I}_0 \quad (3.72)$$

We thus directly can read-off both the response coefficient $\chi_{IF} = 4/\sqrt{\kappa}$ of the detector (which is frequency independent as we focus on $\omega \ll \kappa$), and the intrinsic imprecision noise in the output \hat{I}_0 .

We see that two orthogonal (and hence canonically conjugate) quadratures of the input noise \hat{d}_{in} entering the cavity determine the two kinds of relevant noise (back-action and imprecision). This is to be expected: it is fluctuations in the amplitude quadrature of the incident drive that cause photon number fluctuations and hence back-action, while it is the phase quadrature fluctuations which give imprecision noise.

3.8.1 Vacuum noise input

Taking the input noise to be vacuum noise and using Eqs. (2.10),(2.11), it is straightforward to calculate the needed noise correlators:

$$\bar{S}_{FF}[\omega] = \frac{4\hbar^2}{\kappa}, \quad \bar{S}_{II}[\omega] = 1 \quad \bar{S}_{IF}[\omega] = 0 \quad (3.73)$$

Note crucially that there are no correlations between back-action and imprecision noise, as they correspond to conjugate quadratures of the input vacuum noise. The vanishing of correlations can ultimately be traced back to the fact that averages like $\langle \hat{d}_{\text{in}}(t)\hat{d}_{\text{in}}^\dagger(t') \rangle$ are always zero in the vacuum state.

It thus follows that:

$$\bar{S}_{zz}\bar{S}_{FF} \equiv \frac{\bar{S}_{II}\bar{S}_{FF}}{\chi_{IF}^2} = \frac{4\hbar^2/\kappa}{16/\kappa} = \frac{\hbar^2}{4} \quad (3.74)$$

Our driven cavity thus optimizes the quantum noise inequality of Eq. (3.37), but has no back-action-imprecision correlations. From our general discussion, this implies that it is able to reach the quantum limit on the added noise exactly at the mechanical resonance, but away from resonance, misses the true quantum limit by a large amount.

³There is in principle a proportionality constant between \hat{I} and the phase quadrature of the output field; however, this constant plays no role in determining the detector added noise, so we set it to unity.

30 Quantum limit on continuous position detection

In the case where one wishes to reach the quantum limit on resonance, it is interesting to ask what the optimal coupling strength is using Eq. (3.56). It is convenient to parameterize the coupling in terms of the cooperativity \mathcal{C} , defined as:

$$\mathcal{C} \equiv \frac{4G^2}{\kappa\gamma} \quad (3.75)$$

The optimal coupling required to reach the quantum limit on resonance then becomes:

$$\mathcal{C}_{\text{opt}} = \frac{1}{4} \quad (3.76)$$

3.8.2 Noise correlations via “variational” readout

As we have seen, reaching the quantum limit in the free mass limit (i.e. at frequencies much larger than ω_M) requires strong correlations between the back-action noise in \hat{F} and the imprecision noise in \hat{I}_0 , c.f. Eq. (3.63). These correlations are absent in the simplest scheme described above, as the back-action and imprecision noise operators correspond to conjugate quadratures of the input vacuum noise.

An extremely simple way to induce correlations between back-action and imprecision is to alter the choice of which quadrature of the cavity output field to measure. Suppose instead of the choice in Eq. (3.71), we chose to measure the output quadrature:

$$\hat{I}_{\text{new}} \equiv i \left(e^{i\varphi} \hat{d}_{\text{out}} - e^{-i\varphi} \hat{d}_{\text{out}}^\dagger \right) = \cos \varphi \hat{I}_{\text{old}} - \sin \varphi \left(\frac{\hat{F}}{2\hbar/\sqrt{\kappa}} \right) \quad (3.77)$$

where the angle φ determines the particular choice of quadrature. $\varphi = 0$ corresponds to the measuring the phase quadrature as before, and ensures that \hat{I} has a maximal sensitivity to \hat{x} (as \hat{x} only appears in the imaginary part of \hat{d}_{out} , c.f. Eq. (3.68)). By taking $\varphi \neq 0$, we reduce the response coefficient χ_{IF} , but trivially induce back-action - imprecision correlations, as now the measured detector output *includes* explicitly the back-action fluctuations \hat{F} . For an arbitrary choice of φ , one finds that \bar{S}_{FF} and \bar{S}_{II} are unchanged from Eq. (3.73), but:

$$\chi_{IF} = \frac{4 \cos \varphi}{\sqrt{\kappa}} \quad \bar{S}_{IF}[\omega] = -\sin \varphi \frac{2\hbar}{\sqrt{\kappa}} \quad (3.78)$$

The detector still saturates the Heisenberg bound on its quantum noise:

$$\bar{S}_{zz} \bar{S}_{FF} - \bar{S}_{zF}^2 \equiv \frac{\bar{S}_{II} \bar{S}_{FF} - \bar{S}_{IF}^2}{\chi_{IF}^2} = \frac{(4\hbar^2/\kappa)(1 - \sin^2 \varphi)}{16 \cos^2 \varphi / \kappa} = \frac{\hbar^2}{4} \quad (3.79)$$

Thus, this strategy in principle allows one to reach the quantum limit on the added noise for frequencies away from mechanical resonance, where one requires a non-zero cross-correlator. In the free-mass limit $\omega \gg \omega_M$, the optimal value of \bar{S}_{zF} is given by Eq. (3.63). Achieving this value requires:

$$\frac{\hbar}{2} \tan \varphi = \frac{\omega}{\gamma} \quad (3.80)$$

One sees that the required choice of φ is frequency dependent. To achieve the optimal correlations over a finite range of frequencies, one could first apply a frequency-dependent rotation to the output field from the optomechanical cavity (using, e.g. a

second detuned cavity), and then measure a fixed quadrature. Perhaps more troubling is the fact that the RHS of the above equation is typically extremely large, implying that $\varphi \rightarrow \pi/2$. In this limit, the measured output quantity is almost equivalent to the amplitude quadrature of the input noise incident on the cavity, and has almost no information on the state of the mechanics.

The above approach is known as the “variational” readout strategy in the gravitational wave detection community (Vyatchanin and Zubova, 1995; Vyatchanin and Matsko, 1996), and is also discussed (in a slightly different way) in the lectures of Yanbei Chen. While this seems like a simple strategy for reaching the quantum limit away from mechanical resonance, in practice it is not a good strategy: the strong reduction in the size of the signal means that even though the intrinsic detector noise may be as small as required by quantum mechanics, other non-intrinsic sources of added noise will start to dominate. In short, reaching the quantum limit by throwing away signal strength is almost never a good strategy.

3.8.3 Noise correlations via squeezing

We would like to find a way to induce the needed noise correlations for reaching the quantum limit away from mechanical resonance, while at the same time not modifying the size of the measured signal in the output of our detector. The trick will be to modify the input noise driving the cavity. It is convenient to introduce canonical (Hermitian) quadratures of the input noise $d_{\text{in}}(t)$ via:

$$\hat{d}_{\text{in}} = \frac{1}{\sqrt{2}} \left(\hat{X}_{\text{in}} + i\hat{Y}_{\text{in}} \right) \quad (3.81)$$

As we have seen, back-action is controlled by \hat{X}_{in} and imprecision noise by \hat{Y}_{in} . A straightforward calculation shows that

$$\bar{S}_{zF} = \hbar \bar{S}_{Y_{\text{in}}, X_{\text{in}}} \quad (3.82)$$

Hence, back-action imprecision noise correlations require a state where the fluctuations in the two quadratures of the input noise are strongly correlated. Further, we still require that the quantum noise inequality of Eq. (3.37) be saturated, even in the presence of strong correlations. The required input noise corresponds to a quantum squeezed state (see, e.g., (Gerry and Knight, 2005) for an extensive discussion). In phase space, the Wigner function of such a state has elliptical iso-probability contours (as opposed to the circular contours of a vacuum state or thermal state). The elongated direction of the ellipse should be aligned so as to yield the desired large correlations. As the needed correlations should be negative, the “squeezed” direction of the ellipse (direction with minimal fluctuations) corresponds to the quadrature:

$$\tilde{X}_{\text{in}} = \frac{1}{\sqrt{2}} \left(\hat{X}_{\text{in}} + \hat{Y}_{\text{in}} \right) \quad (3.83)$$

For a squeezed state where \tilde{X} is the squeezed quadrature, we have:

$$\bar{S}_{\tilde{X}_{\text{in}} \tilde{X}_{\text{in}}} = \frac{1}{2} e^{-2r} \quad (3.84)$$

32 Quantum limit on continuous position detection

where $r \geq 0$ is the squeeze parameter. Reaching the quantum limit at a frequency $\omega \gg \omega_M$ with our cavity detector thus requires one to use an input squeezing with a squeezing magnitude

$$e^{-2r} = \frac{\gamma}{2\omega}. \quad (3.85)$$

The idea of using squeezing to generate strong back-action-imprecision correlations was discussed extensively in (Pace, Collett and Walls, 1993) (albeit using a somewhat different formulation), and is also discussed in the lectures of Y. Chen. We stress that the use of squeezing is to generate correlations; it is *not* being used to make up for a lack of incident laser power (i.e. \bar{a}_{cl} too small).

An alternate use of squeezing which *is* equivalent to tuning the incident optical power was discussed in the seminal work (Caves, 1981). Imagine one wants to reach the quantum limit at mechanical resonance, but cannot achieve the optical power required to balance the contributions from back-action and imprecision noises, i.e. achieve the condition in Eq. (3.76). Squeezing can help in this situation. If one squeezes the phase quadrature of the incident light \hat{Y}_{in} (and thus necessarily amplifies the amplitude quadrature \hat{X}_{in}), the back-action noise is enhanced, and the imprecision noise reduced. Hence, input squeezing in this case is equivalent to boosting the magnitude of the cavity drive, i.e. increasing the cooperativity \mathcal{C} . Squeezing in this case does not generate any back-action-imprecision correlations.

4

Backaction evasion and conditional squeezing

In this chapter, we discuss a method for monitoring mechanical position that is not subject to any fundamental quantum limit. As the quantum limit of the previous chapter is indeed a true, unavoidable limit, the only way to do better is to somehow change the rules of the game. Here, this is accomplished by being more modest in what we choose to measure. Recall that a standard weak, continuous position measurement one attempts to measure both quadrature components of the mechanical motion. i.e. $X(t)$ and $Y(t)$ as defined in Eq. (4.1). Quantum mechanically these are conjugate, non-commuting observables; as a result, one cannot measure both quadratures perfectly, as the measurement of X perturbs Y (and vice-versa). In this chapter, we will give up trying to have full knowledge of $x(t)$, and will instead attempt to monitor only one of the two quadrature components. As we will show, this is something that can be done with no fundamental limit coming from quantum mechanics. This opens the door to force sensing with no fundamental quantum limit, as well as the possibility of using the measurement to generate quantum squeezed states of the mechanical resonator. The classic reference discussing such back-action evading single quadrature measurements are (Braginsky *et al.*, 1980), (Caves *et al.*, 1980) and (Bocko and Onofrio, 1996), while the full quantum theory (including the production of conditional quantum squeezed states) was treated in (Clerk, Marquardt and Jacobs, 2008). Note that several recent experiments have implemented this scheme using microwave circuit realizations of optomechanics: (Hertzberg *et al.*, 2010; Suh *et al.*, 2014; Lecocq *et al.*, 2015).

4.1 Single quadrature measurements

Our goal is measure a single mechanical quadrature. The canonically-conjugate quadrature operators are defined in the Heisenberg picture (with respect to the mechanical Hamiltonian) as:

$$\hat{x}(t) = \left(\sqrt{2}x_{\text{ZPF}}\right) \hat{X}(t) \cos(\omega_{\text{M}}t) + \hat{Y}(t) \sin(\omega_{\text{M}}t). \quad (4.1)$$

with

$$\hat{X} = \frac{1}{\sqrt{2}} \left(\hat{b} + \hat{b}^\dagger\right), \quad \hat{Y} = \frac{-i}{\sqrt{2}} \left(\hat{b} - \hat{b}^\dagger\right) \quad (4.2)$$

We stress that in the Schrödinger picture, $\hat{X}(t)$ and $\hat{Y}(t)$ are explicitly time-dependent observables, and do not simply correspond to the position and momentum operators of the mechanical resonator. For example, in the Schrödinger picture, we have:

34 Backaction evasion and conditional squeezing

$$\hat{X}(t) = \frac{1}{\sqrt{2}} \left(\hat{b} e^{i\omega_M t} + \hat{b}^\dagger e^{-i\omega_M t} \right) = \frac{1}{x_{\text{ZPF}}} \left(\cos(\omega_M t) \hat{x} - \frac{\sin(\omega_M t)}{m\omega_M} \hat{p} \right) \quad (4.3)$$

In the second equality, \hat{x} (\hat{p}) is the standard Schrödinger-picture position (momentum) operator of the oscillator. For an undamped oscillator, both quadrature operators are constants of the motion. Note that the definition of the quadrature operator necessarily requires some external phase reference, or equivalently, some choice defining the zero of time. With the above definition, $\hat{X}(t=0)$ is proportional to the mechanical position, while $\hat{Y}(t=0)$ is proportional to the mechanical momentum.

The goal is to measure say \hat{X} , and have all the corresponding back-action of the measurement drive the unmeasured quantity \hat{Y} . As \hat{X} is dynamically independent of \hat{Y} , the back-action will never come back to corrupt subsequent measurements of \hat{X} at later times, and we can in principle make the measurement better and better by increasing the measurement strength. Such a measurement is known as a back-action evading (BAE) measurement. It is also an example of a quantum non-demolition measurement, as one is measuring an observable (i.e. $\hat{X}(t)$) that is a constant of the motion.

While the basic idea is clear, upon first glance implementation would seem to be a challenge. To measure \hat{X} , we just need to couple this operator to some input operator \hat{F} of our detector. From Eq. (4.3), we see that this would require time-dependent couplings between the detector and *both* the mechanical position \hat{x} and mechanical momentum \hat{p} . This would be extremely difficult to achieve (see, e.g., Y. Chen's lectures discussing the difficulties of coupling a detector to mechanical momentum).

Luckily, there is a simple trick to let us turn a standard coupling between detector and mechanical position (like we have in optomechanics) into the kind of single-quadrature coupling we need. The trick has two parts:

- Start with a detector which couples to mechanical position, but modulate the coupling strength in time at the mechanical frequency ω_M . Working in the Schrodinger picture, we want to modify the basic system-detector interaction in Eq. (3.41) to now have the form:

$$\hat{H}_{\text{int}} = (\bar{A} \cos \omega_M t) \hat{x} \cdot \hat{F} = \hat{X}(t) (1 + \cos 2\omega_M t) + \hat{Y}(t) \sin 2\omega_M t \quad (4.4)$$

In the last line, we have re-expressed things in terms of the quadrature operators. Note that the coupling to \hat{X} has a time-independent part, where the coupling to \hat{Y} is strictly oscillating.

- Next, imagine we work with a “slow” detector, one that cannot respond to perturbations occurring at frequencies $\sim 2\omega_M$. In that case, the time-dependent oscillating terms in the above equation will average away, and we will be left with a time-independent coupling between the detector force operator \hat{F} and the \hat{X} quadrature only.

4.2 Two-tone QND scheme

As first discussed in (Braginsky *et al.*, 1980), the above “modulated” coupling scheme for measuring a single mechanical quadrature can be achieved using a standard optomechanical setup if one works in the resolved sideband regime $\omega_M \gg \kappa$ and drives

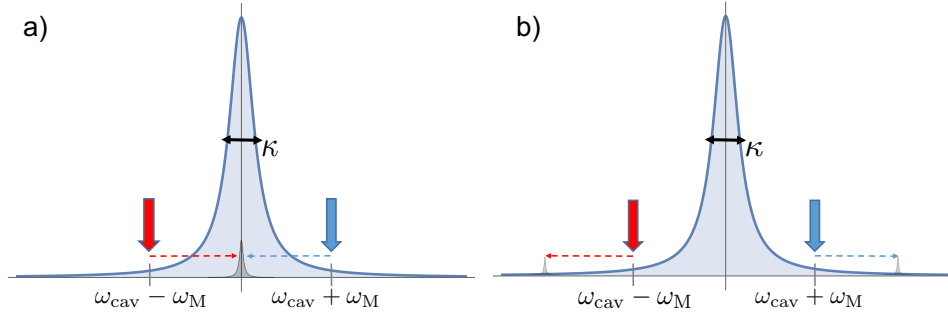


Fig. 4.1 (a) Cavity density of states and drive frequencies for the two-tone BAE measurement scheme; the frequencies of the classical drives are marked with large solid arrows. Photons arriving at the cavity resonance could have been generated either by anti-Stokes scattering from the red-detuned drive tone, or Stokes scattering from the blue-detuned drive tone. As the amplitudes of these drives are equal, the cavity amplitude at resonance effects a measurement of the mechanical X quadrature. One needs to be in the good cavity limit, where the mechanical frequency ω_M is much larger than the cavity linewidth κ . (b) The mechanical motion can also generate weak amplitudes at frequencies $\omega_{\text{cav}} \pm 2\omega_M$ via non-resonant Raman processes. As the density of states for such processes is small, their amplitude is weak. These processes effectively measure the mechanical Y quadrature, and thus causing a small back-action heating of X .

the cavity equally with coherent tones at both the red and blue mechanical sidebands, i.e. at $\omega_{\text{cav}} \pm \omega_M$. This is equivalent to amplitude modulating the laser drive on the cavity. We thus consider a cavity input field (i.e. laser drive) of the form:

$$\bar{a}_{\text{in}}(t) \sim e^{-i\omega_{\text{cav}}t} \sin(\omega_M t + \phi) \quad (4.5)$$

The phase ϕ of the amplitude modulation will directly determine the definition of the mechanical quadrature which couples to the cavity field; we take $\phi = 0$ for simplicity in what follows. As usual, this coherent-state drive will induce an average (time-dependent) amplitude in the cavity $\alpha(t)$ that can be found by solving the classical equations of motion. We will again work in a displaced frame, and thus write the cavity lowering operator as this classical amplitude plus a correction \hat{d} which describes noise effects and the effects of the optomechanical coupling:

$$\hat{a} = \bar{a}_{\text{cl}}(t) + \hat{d}, \quad \bar{a}_{\text{cl}}(t) = \alpha_0 e^{-i\omega_{\text{cav}}t} \cos \omega_M t \quad (4.6)$$

We can take α_0 to be real without loss of generality.

Linearizing the optomechanical interaction in the usual way yields:

$$\hat{H}_{\text{int}} = g \hat{a}^\dagger \hat{a} \frac{\hat{x}}{x_{\text{ZPF}}} \simeq \left[\frac{g}{x_{\text{ZPF}}} \alpha_0 \cos(\omega_M t) \right] \hat{x} \left(\hat{d} e^{i\omega_{\text{cav}}t} + h.c. \right) \quad (4.7)$$

$$\equiv A(t) \hat{x} \cdot \hat{F}(t) \quad (4.8)$$

36 Backaction evasion and conditional squeezing

We see that modulating the average cavity intensity naturally provides the modulated coupling we are after. Working in an interaction picture with respect to the free mechanical and cavity Hamiltonians $\hat{H}_0 = \omega_M \hat{b}^\dagger \hat{b} + \omega_{\text{cav}} \hat{d}^\dagger \hat{d}$ yields

$$\hat{H}_{\text{int}} = \frac{G}{\sqrt{2}} \left[\hat{X} (1 + \cos 2\omega_M t) + \hat{Y} \sin 2\omega_M t \right] (\hat{d} + \hat{d}^\dagger) \quad (4.9)$$

where we have defined the many-photon coupling $G = g\alpha_0$. Note that in our interaction picture, the mechanical quadrature operators have no explicit time-dependence, and are given by Eqs. (4.1).

We now make use of the resolved sideband, good-cavity condition $\omega_M \gg \kappa$, and the fact that we will be interested in coupling $G \ll \kappa$. In this limit the terms oscillating at frequency $2\omega_M$ will average to zero on the timescales relevant to the dynamics (which will all be much longer than $1/\kappa$). We can thus safely make the rotating-wave approximation (RWA), and drop the oscillating terms, resulting in a time-independent interaction Hamiltonian:

$$\hat{H}_{\text{int}} = G \hat{X} \cdot \left(\frac{\hat{d} + \hat{d}^\dagger}{\sqrt{2}} \right) \equiv G \hat{X} \cdot \hat{X}_{\text{cav}} \quad (4.10)$$

We see that the mechanical \hat{X} quadrature is coupled only to the corresponding X quadrature of the cavity. Without dissipation, both \hat{X} and \hat{X}_{cav} are constants of the motion. Similar to the case of standard position detection, as the mechanics only couples to the X cavity quadrature, information on its motion will only drive the conjugate cavity quadrature $\hat{Y} \sim -i(\hat{d} - \hat{d}^\dagger)$ (i.e. the optical phase quadrature). By measuring the output Y quadrature, we thus obtain a measurement of the mechanical \hat{X} quadrature.

To see this explicitly, we first solve the Heisenberg Langevin equation for \hat{d} :

$$\frac{d}{dt} \hat{d}(t) = -\frac{\kappa}{2} \hat{d}(t) - \frac{iG}{\sqrt{2}} \hat{X}(t) - \sqrt{\kappa} \hat{d}_{\text{in}}(t) \quad (4.11)$$

Information on the mechanics will be at the cavity field near resonance, in a bandwidth $\sim \gamma \ll \kappa$. We thus only need to describe \hat{d} at frequencies $\ll \kappa$, and solve this equation adiabatically, i.e. ignoring the d/dt term. This yields:

$$\hat{d}(t) = \frac{-2iG}{\sqrt{2}\kappa} \hat{X}(t) - \frac{2}{\sqrt{\kappa}} \hat{d}_{\text{in}}(t) \quad (4.12)$$

Information on the mechanical X quadrature is, as expected, encoded solely in the imaginary part of \hat{d} , and hence in the cavity Y quadrature. One thus measures the Y quadrature of the output field. The measurement output (i.e. output homodyne current) is then:

$$\hat{I}(t) = \sqrt{2} \hat{Y}_{\text{cav, out}} \sim \sqrt{2\kappa} \hat{Y}_{\text{cav}} \sim \frac{2\sqrt{2}G}{\sqrt{\kappa}} \hat{X}(t) + \hat{\xi}(t) \quad (4.13)$$

$$\equiv \frac{2\sqrt{2}G}{\sqrt{\kappa}} \left(\hat{X}(t) + \delta \hat{X}_{\text{imp}}(t) \right) \quad (4.14)$$

where $\hat{\xi} = -i(\hat{d}_{\text{in}} - \hat{d}_{\text{in}}^\dagger)$ is the Y quadrature of the input noise driving the cavity, and is delta-correlated. In the last line, we have introduced the imprecision noise operator $\delta\hat{X}_{\text{imp}}(t)$ in the usual way, by referring the intrinsic noise in $\hat{I}(t)$ back to the measured mechanical quadrature. Note the $\sqrt{2}$ factor in the definition of the homodyne current has just been included for convenience (the overall prefactor plays no role in our analysis).

Using this form, one easily finds that symmetrized spectral density of the imprecision noise is given by:

$$\bar{S}_{XX,\text{imp}}[\omega] = \frac{\kappa}{8G^2} \equiv \frac{1}{\tilde{k}} \quad (4.15)$$

The imprecision noise spectral density has the units of an inverse rate, and we have thus used it to define an effective measurement rate \tilde{k} .

The rate \tilde{k} has a simple interpretation: it tells us how quickly the power signal-to-noise (SNR) ratio grows for a measurement where we try to resolve whether the measured mechanical quadrature has been displaced an amount $\sim x_{\text{ZPF}}$, i.e. is $X = 1$ or 0? A simple estimator would be to simply integrate the output current $I(t)$, i.e.

$$\hat{m}(t) \equiv \int_0^t dt' \hat{I}(t') \quad (4.16)$$

It is easy to then check that in the absence of mechanical dissipation (and to lowest order in the coupling to the detector)

$$\text{SNR} \equiv \frac{\text{signal power}}{\text{noise power}} = \frac{[\langle \hat{m}(t) \rangle_{X=1} - \langle \hat{m}(t) \rangle_{X=0}]^2}{\langle \langle \hat{m}^2(t) \rangle \rangle} = \frac{(\sqrt{\tilde{k}t} - 0)^2}{t} = \tilde{k}t \quad (4.17)$$

where the variance $\langle \langle \hat{m}^2(t) \rangle \rangle = \langle \hat{m}^2(t) \rangle - \langle \hat{m}(t) \rangle^2$.

Having understood the basics of the measurement, we can now ask about the effects of back-action. Consider first the ideal limit where $\kappa/\omega_M \rightarrow 0$, and hence the cavity has strictly no coupling to the mechanical \hat{Y} quadrature. In this case \hat{X} commutes with the interaction Hamiltonian, implying that it is completely unaffected by the coupling. By solving the mechanical Heisenberg-Langevin equation, one finds that the fluctuations are the same as when $G = 0$, i.e.

$$\bar{S}_{XX}[\omega] \equiv \frac{1}{2} \int_{-\infty}^{\infty} dt e^{i\omega t} \langle \{ \hat{X}(t), \hat{X}(0) \} \rangle = \frac{\gamma/2}{\omega^2 + (\gamma/2)^2} (1 + 2\bar{n}_{\text{th}}^M) \quad (4.18)$$

Again, this is exactly what we would have without any coupling to the cavity.

In contrast, the mechanical Y quadrature is driven by the fluctuations in the cavity \hat{X}_{cav} operator. This back-action does not change the damping rate of the quadrature, but does heat it an amount corresponding to \bar{n}_{BA} quanta. One finds:

$$\bar{S}_{YY}[\omega] = \frac{\gamma/2}{\omega^2 + (\gamma/2)^2} (1 + 2\bar{n}_{\text{th}}^M + 2\bar{n}_{\text{BA}}), \quad \bar{n}_{\text{BA}} = \frac{2G^2}{\kappa\gamma} \equiv \mathcal{C} \quad (4.19)$$

We have introduced here again the optomechanical cooperativity \mathcal{C} , which in this context, can be viewed as the ratio of the measurement rate to the intrinsic mechanical damping rate.

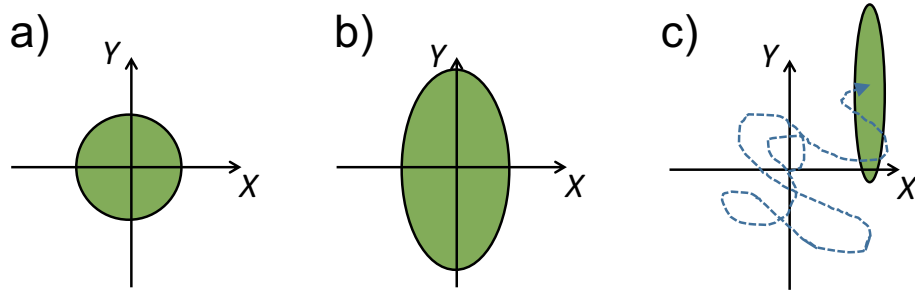


Fig. 4.2 Mechanical state associated with various aspects of the BAE measurement, depicted as probability density in the phase space associated with the mechanical quadrature amplitudes X and Y . (a) Mechanical state without the measurement: a thermal state with equal uncertainty in the X and Y quadratures. (b) Unconditional mechanical state when the measurement is on. The measured X quadrature is unaffected by the measurement, whereas the back-action of the measurement heats the Y quadrature and thus increases its uncertainty. (c) Conditional mechanical state. If we use the information in the measurement record $I(t)$ associated with a particular run of the experiment, we see that the mechanical resonator is in a squeezed state, where the X quadrature uncertainty has been greatly reduced compared to its original value. However, the mean values of X and Y (i.e. centre of the ellipse) undergoes a random walk which is completely correlated with the measurement record. If we average over these fluctuations (e.g. discard the measurement record), we recover the picture in panel (b).

What if we include the effects of κ/ω_M ? The oscillating terms in Eq. (4.9) are now not completely negligible. Heuristically, they give rise to scattering processes where incident drive photons are scattered to frequencies $\omega_{\text{cav}} \pm 2\omega_M$ (see Fig. 4.1 (b)). Such processes have a very small amplitude due to the very small cavity density of states at these frequencies. They do however contain information on the mechanical Y quadrature, thus result in heating of the mechanical X quadrature. A careful calculation (see (Clerk *et al.*, 2008)) finds that this additional heating results can be captured by making the replacement:

$$\bar{n}_{\text{th}}^M \rightarrow \bar{n}_{\text{th}}^M + \frac{1}{32} \left(\frac{\kappa}{\omega_M} \right)^2 \quad (4.20)$$

in Eqs. (4.18),(4.19) for the quadrature noise spectral densities

4.3 Conditional squeezing: heuristic description

We have seen that a perfect back-action evading measurement results in a heating of the unmeasured, conjugate mechanical quadrature Y , while the measured mechanical quadrature X is completely unaffected by the measurement, c.f. Eq. (4.18). This is in keeping with the fact that \hat{X} commutes with the optomechanical coupling Hamiltonian, and is thus completely unaffected by the light field used for the measurement. We thus expect the mechanical state (pictured as a phase space distribution) to be modified

as shown in Fig. 4.2(b). Note that the total entropy of the state appears to have been increased by the measurement.

While this seems simple enough, it would seem to contradict another aspect of our treatment. Namely, we showed that the added noise of the measurement (which has no back-action contribution) could be made arbitrarily small by increasing the measurement strength (i.e. G), meaning that one could make an essentially perfect measurement of X . This seems to imply that the measurement will greatly reduce the uncertainty in the X quadrature, in stark contrast to what is depicted in Fig. 4.2(b).

There is of course no contradiction here. To fully describe the reduction in X uncertainty occurring during a measurement, we need to understand what happens during a particular run of the experiment: given a particular history of the measurement output $I(t)$, what is the state of the mechanical resonator? We will show that there is a particularly simple picture for this “conditional” mechanical state, as is shown schematically in Fig. 4.2(c). Once transients have died away, the conditional mechanical state will have greatly reduced X quadrature uncertainty— it will be a squeezed state. However, the mean position of this state in phase space will undergo a random walk, a random walk which is completely correlated with the seemingly random fluctuations of the measurement record $I(t)$. If we have access to the measurement record, we can follow these fluctuations, and thus to us, this random motion does not represent a true uncertainty.

In contrast, for an observer who does not have access to $I(t)$, the fluctuations in the mean position of the mechanical squeezed state are just another uncertainty in the mechanical state. For such an observer, the mechanical resonator is best described by the unconditional state, where we average over all possible measurement outcomes, and thus include the random walk done by the conditional squeezed state means in the state uncertainty. Doing so, we return to the picture in Fig. 4.2(b): the fluctuations in the mechanical resonator X quadrature to an observer who does not have access to the measurement record are the same as they were without the measurement.

In what follows, we will develop in more detail the theoretical tools required to describe such a conditional evolution and the conditional mechanical state. We will then apply this formalism to our optomechanical back-action evading measurement to understand how one can generate squeezed mechanical states from the measurement.

4.4 Stochastic master equation description of a conditional measurement

In this section, we will give a quick and dirty “derivation” of the stochastic master equation approach that describes the conditional evolution of the mechanical state during an ideal version of our back-action evading measurement. Our approach follows closely the extremely pedagogical treatment in (Jacobs and Steck, 2006), which itself is related to the derivation in (Caves and Milburn, 1987). The derivation, interpretation and use of such stochastic master equations are treated extensively in recent textbooks (Wiseman and Milburn, 2014; Jacobs, 2014).

4.4.1 Discretized measurement record

We start by writing the measurement output (Eq. (4.14)) as

$$\hat{I}(t) = \sqrt{\bar{k}}\hat{X}(t) + \hat{\xi}(t) \quad (4.21)$$

As we already saw in the discussion surrounding Eq. (4.17), if we only look at $I(t)$ over a very short time interval, we get almost no information on the state of the mechanical resonator: the noise $\xi(t)$ in the measurement record completely dominates the contribution from the signal $X(t)$. Useful information is thus only acquired gradually over time. To describe our measurement, we want to quantitatively describe the small information gain that occurs over a given short time interval, and importantly, also describe the corresponding change in the mechanical state.

We start by discretizing time into finite intervals of width Δt and define $t_j \equiv j\Delta t$; we will eventually take the $\Delta t \rightarrow 0$ limit. During each of these finite intervals, we use the information in $I(t)$ to estimate the state of the mechanics. This is done analogously to Eq. (4.17). The estimate of X derived from $I(t)$ in the interval (t_{j-1}, t_j) is described by the operator \hat{X}_{t_j} , defined as

$$\hat{X}_{t_j} \equiv \frac{1}{\sqrt{\bar{k}\Delta t}} \int_{t_{j-1}}^{t_j} dt' \hat{I}(t'). \quad (4.22)$$

For simplicity, we start by assuming that the instantaneous mechanical resonator state is pure and described by the wavefunction $|\psi(t)\rangle$, and assume that it has no intrinsic dynamics— we ignore its intrinsic dissipation and any external forces. We will also assume that any back-action disturbance occurs instantaneously at the end of each interval (t_{j-1}, t_j) , and hence $|\psi(t)\rangle$ is constant over the interval. As we are interested in the $\Delta t \rightarrow 0$ limit, this approximation is not unreasonable. Using this fact and the fact that $\langle \hat{\xi}(t) \rangle = 0$, we have

$$\langle \hat{X}_{t_j} \rangle \simeq \langle \hat{X}(t) \rangle \equiv \langle \psi(t) | \hat{X} | \psi(t) \rangle \quad (4.23)$$

We can also calculate the variance of \hat{X}_{t_j} :

$$\begin{aligned} \left\langle \left\langle \left(\hat{X}_{t_j} \right)^2 \right\rangle \right\rangle &\equiv \left\langle \left(\hat{X}_{t_j} - \langle \hat{X}_{t_j} \rangle \right)^2 \right\rangle \\ &\simeq \frac{1}{\left(\sqrt{\bar{k}\Delta t} \right)^2} \int_{t_{j-1}}^{t_j} dt' \int_{t_{j-1}}^{t_j} dt'' \langle \hat{\xi}(t') \hat{\xi}(t'') \rangle \end{aligned} \quad (4.24)$$

$$= \frac{1}{\bar{k}\Delta t} \equiv \sigma \quad (4.25)$$

Note that we have ignored the contribution to the variance from the intrinsic uncertainty of \hat{X} in the mechanical resonator state $|\psi(t)\rangle$. This is because the contribution we keep (which is solely from the imprecision noise of the measurement, $\xi(t)$) completely dominates the intrinsic noise in the limit of small Δt . This imprecision-noise contribution scales like $1/\Delta t$, while the intrinsic noise would tend to a constant.

We have thus discretized the measurement record $I(t)$ that would be obtained in a given experimental run into a set of discrete X -quadrature estimates X_{t_j} . These estimates can be viewed as an effective classical stochastic process, i.e.

$$X_{t_j} = \langle \hat{X}(t_j) \rangle + \frac{\Delta W_j}{\sqrt{k\Delta t}} \quad (4.26)$$

Here, the ΔW_j are random variables describing the fluctuations of each estimate due to the imprecision noise $\xi(t)$ in the measurement record. Equivalently, they represent the difference in the outcome of the measurement during the given time interval from the mean of \hat{X} in the state $|\psi(t)\rangle$. As $\xi(t)$ is Gaussian white noise, it follows that the ΔW_j are each Gaussian random variables with zero mean, and further, are not correlated with one another. From Eq. (4.25), we have simply:

$$\overline{\Delta W_j} = 0 \quad \overline{\Delta W_j \Delta W_{j'}} = \delta_{j,j'} \Delta t \quad (4.27)$$

The bar here represents an average over the classical stochastic process. We stress that the classical stochastic process defined by Eq. (4.26) has been constructed so that it yields the same statistics as the microscopic (quantum) theory describing our measurement.

4.4.2 State evolution

Having come up with a simple way to think about the measurement record produced in a single run of the experiment, we now return to the question of back-action: in a particular run of the experiment (described by a particular set of X_{t_j}), how will the state $|\psi(t)\rangle$ of the mechanical resonator change over time? Again, we are only considering here mechanical dynamics caused by the measurement, and are assuming that these disturbances happen instantaneously between each measurement interval (t_{j-1}, t_j) . At the end of a given measurement interval, the experimentalist will have obtained a particular measurement result X_{t_j} . If the measurement was a simple, strong projective measurement, the mechanical state after the measurement would be completely determined by the outcome X_{t_j} —the mechanics would just be projected into the eigenstate of \hat{X} corresponding to this outcome.

In our system, we are however very far from the strong measurement limit, as we only obtain a tiny bit of information on X during the given time interval. The final mechanical state will thus depend *both* on the initial mechanical state and the measurement outcome, and we can write:

$$|\psi(t_j + \Delta t)\rangle = \hat{M}(X_{t_j}) |\psi(t_j)\rangle \quad (4.28)$$

The operator $\hat{M}(X_{t_j})$ describes the outcome-dependent disturbance of the mechanical state by the measurement in a given time interval. It is a so-called Krauss operator, used in the POVM description of the kind of incomplete, weak measurements relevant here (see, e.g., (Jacobs and Steck, 2006) for a more complete discussion). We assume the ideal case where this state disturbance is as small as possible given the information gain of the measurement. As the statistics of our measurement outcomes are Gaussian distributed and dominated by imprecision noise, the corresponding Krauss operators also have a Gaussian form:

$$\hat{M}(x) \propto \exp \left[-\frac{1}{4\sigma^2} (x - \hat{X})^2 \right], \quad (4.29)$$

42 Backaction evasion and conditional squeezing

where $\sigma = 1/(\tilde{k}\Delta t)$ is variance of each discrete measurement (c.f. Eq. (4.25)), and we have dropped a normalization constant. Note that in extreme limit where $\sigma \rightarrow \infty$, $\hat{M}(x) \rightarrow 1$: there is no information obtained in the measurement, and hence no measurement-induced change in the mechanical state. In the opposite case $\sigma \rightarrow 0$, the $\hat{M}(x) \rightarrow |x\rangle\langle x|$, i.e. the Krauss operators become projectors onto eigenstates of \hat{X} , and we recover the standard description of a strong measurement.

Using Eq. (4.26), we can re-express the post-measurement mechanical state in terms of the random variables ΔW_j as:

$$|\psi(t_j + \Delta t)\rangle \propto \exp \left[-\frac{\tilde{k}\Delta t}{4} \hat{X}^2 + \left(\frac{\tilde{k}\Delta t}{2} \langle \hat{X}(t_j) \rangle + \sqrt{\frac{\tilde{k}}{4}} \Delta W_j \right) \hat{X} \right] |\psi(t_j)\rangle, \quad (4.30)$$

where again we have dropped purely constant prefactors affecting the normalization of the state.

Next, as we are interested in the $\Delta t \rightarrow 0$ limit, all the terms in the argument of the above exponential will become small, and we can thus Taylor expand keeping terms to order Δt only. This implies that we need terms that are up to second order in ΔW_j , as this random variable has a variance Δt , and hence a typical size $\sqrt{\Delta t}$. We thus find:

$$|\psi(t_j + \Delta t)\rangle \propto \left[1 - \frac{\tilde{k}\Delta t}{4} \hat{X}^2 + \left(\frac{\tilde{k}\Delta t}{2} \langle \hat{X}(t_j) \rangle + \sqrt{\frac{\tilde{k}}{4}} \Delta W_j \right) \hat{X} + \frac{\tilde{k}}{8} (\Delta W_j)^2 \hat{X}^2 \right] |\psi(t_j)\rangle \quad (4.31)$$

Finally, we want to take the limit where the duration of our small time intervals tends to an infinitesimal, $\Delta t \rightarrow dt$, which will give us a stochastic differential equation for the evolution of the mechanical state. In this limit, we will follow standard convention, and label ΔW as dW , the so-called Wiener increment. In general, one would think that dW^2 is itself a random variable which fluctuates. In the $\Delta t \rightarrow 0$ limit, these fluctuations play no role, and we can rigorously replace dW^2 by its average value, dt (see, e.g., Ch. 3 of (Jacobs, 2010) for a detailed discussion). Using this, and also adding terms to ensure that our state remains normalized, we find:

$$\begin{aligned} d|\psi\rangle &\equiv |\psi(t + dt)\rangle - |\psi(t)\rangle \\ &= \left[-\frac{\tilde{k}}{8} (\hat{X} - \langle \hat{X} \rangle)^2 dt + \sqrt{\frac{\tilde{k}}{4}} (\hat{X} - \langle \hat{X} \rangle) dW \right] |\psi(t)\rangle \end{aligned} \quad (4.32)$$

In the same limit, the measurement record can be represented as:

$$dI \equiv \int_{t-\Delta t}^t I(t') \rightarrow \sqrt{\tilde{k}} \langle \hat{X}(t) \rangle dt + dW \quad (4.33)$$

Several comments are now in order:

- Eq. (4.32) and Eq. (4.33) are coupled stochastic differential equations. The random Wiener increment dW both dictates the evolution of the measurement record and

the evolution of the state of the mechanical resonator. Formally, it tells us that the noise in the measurement record directly reflects changes in the mechanical state.

- Eq. (4.32) is a nonlinear, as the expectation value $\langle \hat{X} \rangle$ on the RHS is of course itself a function of the mechanical state. It should be evaluated using the mechanical state at time t .
- It is useful to interpret the two terms Eq. (4.33) in a manner that connects to Bayesian probabilities. The first term is what we “expect” from our measurement, given our current knowledge of the mechanical state (as represented by $|\psi(t)\rangle$). The second term (dW) represents the “surprise” of our measurement. Just as in Bayesian probabilities, we should update our knowledge of the mechanical state based on this new information. This is exactly the role of the dW term on the RHS of Eq (4.32).

Finally, it is straightforward to calculate the corresponding equation of motion for the density matrix describing the mechanical state, using $\hat{\rho} = |\psi\rangle\langle\psi|$ and Eq. (4.32). As usual, one needs to retain terms to order ΔW^2 , as in the $\Delta t \rightarrow 0$ limit, $\Delta W^2 \rightarrow dW^2 = dt$. One finds:

$$d\hat{\rho}\Big|_{\text{meas}} = -\frac{\tilde{k}}{8} [\hat{X}, [\hat{X}, \hat{\rho}]] dt + \sqrt{\frac{\tilde{k}}{4}} (\hat{X}\hat{\rho} + \hat{\rho}\hat{X} - 2\langle\hat{X}\rangle\hat{\rho}) dW \quad (4.34)$$

Again, the last term on the RHS $\propto dW$ describes how the evolution of mechanical state is correlated with the noise in the measurement record; equivalently, it tells us how our knowledge of the mechanical state (as encoded in $\hat{\rho}$) is updated by the surprise dW of the measurement. Note that if $\hat{\rho}$ is initially in a pure state, then Eq. (4.34) keeps it in a pure state at all times (for the simple reason that the evolution described by Eq. (4.32) also keeps the mechanical state pure). The evolution of the density matrix clearly depends on the particular history and form of the measurement record (through the dW) terms, and we call this the *conditional density matrix*. One could also ask what the state of the mechanical resonator is averaged over *all possible* measurement outcomes. Equivalently, if we don’t have access to $I(t)$, how would we describe the mechanical state? Averaging over possible measurement records is equivalent to averaging over the dW , which is simple, as $dW = 0$. Hence, the *unconditional* density matrix evolves only under the first term on the RHS of Eq. (4.34). As can easily be checked, this term causes off-diagonal elements of the the density matrix in the \hat{X} -eigenstate basis to decay exponentially. This is just the expected unconditional back-action of the measurement, which is a heating of the unmeasured Y quadrature.

Note that while we have given a rather heuristic derivation of the conditional master equation for our system, it is possible to give a more microscopic description, one that starts with the photodetection involved in the homodyne measurement of the cavity output field, see (Clerk *et al.*, 2008) for details.

Finally, we also need to include terms which correspond to the measurement-independent evolution of the mechanical resonator. In our case, the mechanical quadratures have no free Hamiltonian evolution, but will be subject to the heating and damping by the intrinsic sources of mechanical dissipation. We have discussed how these

44 Backaction evasion and conditional squeezing

can be described using the Heisenberg-Langevin formalism. In the Markovian limit of interest, they can equivalently be described by Linblad terms in a quantum master equation:

$$d\hat{\rho}\Big|_{\text{diss}} = \gamma(1 + \bar{n}_{\text{th}}^M) \left[\hat{b}\hat{\rho}\hat{b}^\dagger - \frac{1}{2} \{ \hat{b}^\dagger\hat{b}, \hat{\rho} \} \right] dt + \gamma(\bar{n}_{\text{th}}^M) \left[\hat{b}^\dagger\hat{\rho}\hat{b} - \frac{1}{2} \{ \hat{b}\hat{b}^\dagger, \hat{\rho} \} \right] dt \quad (4.35)$$

These describe the additional and removal of quanta from the mechanical resonator by a thermal reservoir. The total evolution of the system in the presence of the measurement is then:

$$d\hat{\rho} = d\hat{\rho}\Big|_{\text{diss}} + d\hat{\rho}\Big|_{\text{meas}} \quad (4.36)$$

4.5 Conditional back-action evading measurement

We can now apply the general theory of the previous section to our ideal cavity optomechanical single quadrature measurement. We want to describe the conditional state of the mechanical resonator, i.e. its state during a particular run of the measurement, with a particular measurement record $I(t)$. As the RHS of the conditional master equation has no terms that involve more than two mechanical raising or lowering operators, it has the property that Gaussian states (e.g. a thermal state, the ground state) remain Gaussian under the evolution. We can thus reduce our conditional master equation to a set of ODE's for the means and variances of the Gaussian state. For the \hat{X} quadrature, we thus need to know:

$$\bar{X}(t) \equiv \langle \hat{X}(t) \rangle_{\text{cond}} \quad V_X(t) \equiv \langle \hat{X}^2(t) \rangle_{\text{cond}} - \left(\langle \hat{X}(t) \rangle_{\text{cond}} \right)^2 \quad (4.37)$$

where all averages are with respect to the conditional density matrix of the mechanical resonator.

One finds straightforwardly that the evolution of the variances and covariances are completely deterministic, i.e. they do not involve dW . For the X quadrature, one finds:

$$\frac{dV_X}{dt} = -\tilde{k}V_X^2 - \gamma \left(V_X - \bar{n}_{\text{th}}^M - \frac{1}{2} \right) \quad (4.38)$$

This has an extremely simple interpretation. Without the measurement $\tilde{k} = 0$, the intrinsic mechanical dissipation causes V_X to relax exponentially (rate γ) to its thermal equilibrium value. In contrast, with the measurement, the first term tries to relax V_X towards zero, i.e. prepare a squeezed state where the X quadrature variance is minimal.

Note that for our system, the measurement strength $\tilde{k} = 4C\gamma$, where the cooperativity is defined in Eq. (4.19). For the large cooperativity limit, the stationary value of the variance is given by:

$$\frac{V_X}{V_{X,zpt}} \rightarrow \sqrt{\frac{1 + 2\bar{n}_{\text{th}}^M}{2C}} \equiv \sqrt{\frac{1}{2C_{\text{th}}}} \quad (4.39)$$

where in the last line, we have introduced the so-called thermal cooperativity. We thus see that achieving strong quantum squeezing requires $C_{\text{th}} > 1/2$; this is similar to the

condition required for ground state cavity cooling with a system in the good cavity limit.

We can also ask about how we recover the unconditional picture of the measurement, where the X quadrature is unaffected. Recall the picture in Fig. 4.2(c): the X quadrature is in a squeezed state whose mean fluctuates in a way that is correlated with the measurement record. If we don't have access to the measurement record, we should include these fluctuations of the mean in the uncertainty of X , and expect that this will offset the squeezing found before. To make this quantitative, we can calculate the equation of motion for the average of X in the conditional mechanical state from the conditional master equation. One finds:

$$d\bar{X}(t) = -\frac{\gamma}{2}\bar{X}dt + \sqrt{\tilde{k}}V_X(t)dW \quad (4.40)$$

The evolution of the mean of X is indeed fluctuating, in a way that is completely correlated with the measurement record (i.e. dW both determines \bar{X} and the measurement record $I(t)$). If one averages over these fluctuations, one can explicitly check that:

$$V_X + \langle \bar{X}(t)^2 \rangle = \frac{1}{2} + \bar{n}_{\text{th}}^M \quad (4.41)$$

i.e. one recovers the results of the unconditional theory, where the X quadrature variance is the thermal equilibrium value, the same as though there were no measurement.

What about the unmeasured Y quadrature, how does it evolve? Letting $C(t)$ denote the covariance $\frac{1}{2}\langle \{\hat{X}(t), \hat{Y}(t)\} \rangle$, we have again that the remaining variances and covariances also evolve deterministically:

$$\frac{dV_Y}{dt} = -\tilde{k}C^2 - \gamma \left(V_Y - \bar{n}_{\text{th}}^M - \frac{1}{2} \right) + \frac{\tilde{k}}{4} \quad (4.42)$$

$$\frac{dC}{dt} = -\tilde{k}V_X C - \gamma C \quad (4.43)$$

The last term on the RHS of Eq. (4.42) describes the expected heating of the measurement. The first term tells us that if there are correlations between the quadratures, then our measurement of X also has the effect of reducing the uncertainty in Y . Finally, the last equation tells us that under the measurement, any initial correlations between the quadratures will decay away.

Finally, we have considered so far the case of a perfect measurement. It is of course also important to understand what happens to the conditional squeezing generated by the measurement when things are not so perfect. One key imperfection is that the final measurement of the cavity output quadrature is not perfect. This could be due to losses (which replace signal by vacuum noise), or due to unwanted added noise in the final homodyne measurement (e.g. due to a following non-quantum-limited amplifier in a microwave frequency optomechanics experiment). In either case, the next effect is to reduce the size of the signal term in Eq. (4.14) while keeping the noise term the same, i.e. $\tilde{k} \rightarrow \tilde{k}\sqrt{\eta}$, where the efficiency $\eta \leq 1$. Including this imperfection, one finds that the conditioning of the X quadrature (first term in Eq. (4.41)) is reduced by a factor of η , whereas the back-action heating of the Y quadrature is unchanged

(last term in Eq. (4.42)). As a result, in the large cooperativity limit, the condition for quantum squeezing becomes more stringent:

$$\left(\mathcal{C}_{\text{th}} \equiv \frac{2G^2}{\kappa\gamma(1+2\bar{n}_{\text{th}}^M)} \right) \geq \frac{1}{2\eta} \quad (4.44)$$

4.6 Feedback to create unconditional squeezing

As discussed in (Clerk *et al.*, 2008), one can convert the conditional squeezing described above into true squeezing: one needs to use information in the measurement record to apply an appropriate feedback force which suppresses the fluctuations in the conditional mean $\bar{X}(t)$. The feedback force should create an extra damping of the $\bar{X}(t)$; we thus need to apply a linear force which couples to the mechanical \hat{Y} quadrature:

$$\hat{H}_{\text{fb}} = -\alpha \frac{\gamma}{2} \bar{X}(t) \cdot \hat{Y} \quad (4.45)$$

Here, $\alpha(\gamma/2)$ is the strength of the applied feedback. It is easy to check that this feedback force increases the damping of \bar{X} in Eq. (4.40) by an amount $\alpha\gamma/2$. For large α , this feedback-induced damping will suppress the \bar{X} fluctuations, and the unconditional state variance of X will be the same as the conditional (squeezed) variance.

This might still seem mysterious: how does the experimentalist know what $\bar{X}(t)$ is? To answer this, we re-write Eq. (4.40) (including the feedback force) in terms of the measurement record $dI(t)$ defined in Eq. (4.33). We find:

$$\frac{d}{dt}\bar{X} = -\frac{\gamma}{2}(1+\alpha)\bar{X} + \sqrt{\tilde{k}}V_X \left(dI(t) - \sqrt{\tilde{k}}\bar{X} \right) \quad (4.46)$$

We can now solve this equation, expressing $\bar{X}(t)$ in terms of the measurement record at earlier times. Assuming V_X has achieved its stationary value, we have

$$\bar{X}(t) = \sqrt{\tilde{k}}V_X \int_{-\infty}^t dt' e^{-\Gamma(t-t')} dI(t') \quad (4.47)$$

$$\Gamma = \frac{\gamma}{2}(1+\alpha) + \tilde{k}V_X \quad (4.48)$$

Thus, the conditional mean $\bar{X}(t)$ (i.e. our best estimate for the value of the mechanical X quadrature) is determined by filtering the measurement record obtained at earlier times. The optimal filter is just exponentially decaying (i.e. the measurement record at recent times influence our estimate more than the record at earlier times), with a time constant $1/\Gamma$ that depends on both the measurement strength (through \tilde{k}) and on the feedback strength (through α). As has been discussed extensively, the optimal filter here coincides with the classical Kalman filter (see, e.g. (Jacobs, 2014)).

We now have a concrete prescription for how to get unconditional squeezing via measurement plus feedback. At each instant in time, one first constructs the optimal estimate of $\bar{X}(t)$ from the measurement record as per the above equation. Next, one uses this estimate to apply the appropriate linear feedback force which damps \bar{X} . More details on feedback-induced squeezing in this system are provided in (Clerk *et al.*, 2008).

4.7 Extensions of back-action evasion techniques

More elaborate versions of back-action evasion measurements in quantum optomechanics are possible. In a system where two mechanical resonators are coupled to a single cavity, one can extend the two-tone driving approach to make a back-action free measurement of two commuting collective mechanical quadratures (Woolley and Clerk, 2013) (e.g. the sum of the X quadratures of mechanical resonator 1 and 2, and the difference of their Y quadratures). This allows the possibility to measure both quadratures of an applied force with absolutely no quantum limit; it is intimately connected to ideas developed in (Tsang and Caves, 2010) and (Wasilewski *et al.*, 2010).

Another interesting possibility is to “break” the QND measurement described in the previous sections by slightly imbalancing the amplitudes of the two cavity drive tones. This imbalance ruins the back-action evasion nature of the measurement, as the mechanical X quadrature no longer commutes with the Hamiltonian. However, the resulting measurement backaction on X can be harnessed to directly squeeze the mechanical resonator. As discussed extensively in (Kronwald *et al.*, 2013), this is an example of coherent feedback, where the driven cavity both “measures” the mechanical X quadrature, and also applied exactly the correct feedback force needed to squeeze the mechanical resonator. This coherent feedback approach has the strong advantage of not requiring the experimentalist both to make a shot-noise limited measurement of the cavity output, nor to process a classical measurement record and generate an ideal feedback force. In a sense, the driven cavity does all the work. This scheme has been implemented in three recent experiments to achieve true quantum squeezing, where the X -quadrature mechanical uncertainty drops below the zero-point value (even though one starts from a thermal state) (Wollman *et al.*, 2015; Pirkkalainen *et al.*, 2015; Lecocq *et al.*, 2015). This general idea of coherent feedback can also be extended to the “two-mode” backaction-evasion scheme described above, thus providing a means for generating mechanical entanglement (Woolley and Clerk, 2014).

Appendix A

Derivation of power gain expression

To be able to say that our detector truly amplifies the motion of the oscillator, it is not sufficient to simply say the response function χ_{IF} must be large (note that χ_{IF} is not dimensionless!). Instead, true amplification requires that the *power* delivered by the detector to a following amplifier be much larger than the power drawn by the detector at its input— i.e., the detector must have a dimensionless power gain $G_P[\omega]$ much larger than one. If the power gain was not large, we would need to worry about the next stage in the amplification of our signal, and how much noise is added in that process. Having a large power gain means that by the time our signal reaches the following amplifier, it is so large that the added noise of this following amplifier is unimportant

To make the above more precise, we start with the ideal case of no reverse gain, $\chi_{FI} = 0$. We will define the power gain $G_P[\omega]$ of our generic position detector in a way that is analogous to the power gain of a voltage amplifier. Imagine we drive the oscillator we are trying to measure (whose position is x) with a force $2F_D \cos \omega t$; this will cause the output of our detector $\langle \hat{I}(t) \rangle$ to also oscillate at frequency ω . To optimally detect this signal in the detector output, we further couple the detector output I to a second oscillator with natural frequency ω , mass M , and position y : there is a new coupling term in our Hamiltonian, $H'_{int} = B\hat{I} \cdot \hat{y}$, where B is a coupling strength. The oscillations in $\langle I(t) \rangle$ will now act as a driving force on the auxiliary oscillator y (see Fig 3.1). We can consider the auxiliary oscillator y as a “load” we are trying to drive with the output of our detector.

To find the power gain, we need to consider both P_{out} , the power supplied to the output oscillator y from the detector, and P_{in} , the power fed into the input of the amplifier. Consider first P_{in} . This is simply the time-averaged power dissipation of the input oscillator x caused by the back-action damping $\gamma_{BA}[\omega]$. Using a bar to denote a time average, we have

$$P_{in} \equiv M\gamma_{BA}[\omega] \cdot \overline{\dot{x}^2} = M\gamma_{BA}[\omega]\omega^2 |\chi_{xx}[\omega]|^2 F_D^2. \quad (\text{A.1})$$

Note that the oscillator susceptibility $\chi_{xx}[\omega]$ includes the effects of γ_{BA} , c.f. Eq. (3.52).

Next, we need to consider the power supplied to the “load” oscillator y at the detector output. This oscillator will have some intrinsic, detector-independent damping γ_{ld} , as well as a back-action damping γ_{out} . In the same way that the back-action damping γ_{BA} of the input oscillator x is determined by the quantum noise in \hat{F} (cf. Eq. (3.20)), the back-action damping of the load oscillator y is determined by the quantum noise in the output operator \hat{I} :

$$\begin{aligned}\gamma_{\text{out}}[\omega] &= \frac{B^2}{M\omega} [-\text{Im } \chi_{II}[\omega]] \\ &= \frac{B^2}{M\hbar\omega} \left[\frac{S_{II}[\omega] - S_{II}[-\omega]}{2} \right],\end{aligned}\quad (\text{A.2})$$

where χ_{II} is the linear-response susceptibility which determines how $\langle \hat{I} \rangle$ responds to a perturbation coupling to \hat{I} :

$$\chi_{II}[\omega] = -\frac{i}{\hbar} \int_0^\infty dt \left\langle \left[\hat{I}(t), \hat{I}(0) \right] \right\rangle e^{i\omega t}.\quad (\text{A.3})$$

As the oscillator y is being driven on resonance, the relation between y and I is given by $y[\omega] = \chi_{yy}[\omega]I[\omega]$ with $\chi_{yy}[\omega] = -i[\omega M\gamma_{\text{out}}[\omega]]^{-1}$. From conservation of energy, we have that the *net* power flow into the output oscillator from the detector is equal to the power dissipated out of the oscillator through the intrinsic damping γ_{ld} . We thus have

$$\begin{aligned}P_{\text{out}} &\equiv M\gamma_{\text{ld}} \cdot \overline{\dot{y}^2} \\ &= M\gamma_{\text{ld}}\omega^2 |\chi_{yy}[\omega]|^2 \cdot |BA\chi_{IF}\chi_{xx}[\omega]F_D|^2 \\ &= \frac{1}{M} \frac{\gamma_{\text{ld}}}{(\gamma_{\text{ld}} + \gamma_{\text{out}}[\omega])^2} \cdot |BA\chi_{IF}\chi_{xx}[\omega]F_D|^2.\end{aligned}\quad (\text{A.4})$$

Using the above definitions, we find that the ratio between P_{out} and P_{in} is independent of γ_0 , but depends on γ_{ld} :

$$\frac{P_{\text{out}}}{P_{\text{in}}} = \frac{1}{M^2\omega^2} \frac{A^2 B^2 |\chi_{IF}[\omega]|^2}{\gamma_{\text{out}}[\omega] \gamma_{\text{BA}}[\omega]} \frac{\gamma_{\text{ld}}/\gamma_{\text{out}}[\omega]}{(1 + \gamma_{\text{ld}}/\gamma_{\text{out}}[\omega])^2}.\quad (\text{A.5})$$

We now define the detector power gain $G_P[\omega]$ as the value of this ratio maximized over the choice of γ_{ld} . The maximum occurs for $\gamma_{\text{ld}} = \gamma_{\text{out}}[\omega]$ (i.e. the load oscillator is “matched” to the output of the detector), resulting in:

$$\begin{aligned}G_P[\omega] &\equiv \max \left[\frac{P_{\text{out}}}{P_{\text{in}}} \right] \\ &= \frac{1}{4M^2\omega^2} \frac{A^2 B^2 |\chi_{IF}|^2}{\gamma_{\text{out}} \gamma_{\text{BA}}} \\ &= \frac{|\chi_{IF}[\omega]|^2}{4\text{Im } \chi_{FF}[\omega] \cdot \text{Im } \chi_{II}[\omega]}\end{aligned}\quad (\text{A.6})$$

In the last line, we have used the relation between the damping rates $\gamma_{\text{BA}}[\omega]$ and $\gamma_{\text{out}}[\omega]$ and the linear-response susceptibilities $\chi_{FF}[\omega]$ and $\chi_{II}[\omega]$, c.f. Eq. (3.24). We thus find that the power gain is a simple dimensionless ratio formed by the three different response coefficients characterizing the detector, and is independent of the coupling constants A and B . As we will see, it is completely analogous to the power gain of a voltage amplifier, which is also determined by three parameters: the voltage gain, the input impedance and the output impedance.

50 Derivation of power gain expression

Finally, we note that the above results can be generalized to include a non-zero detector reverse gain, χ_{FI} , see (Clerk *et al.*, 2010). In the case of a perfectly symmetric detector (i.e. $\chi_{FI} = \chi_{IF}^*$), one can show that the power gain is at most equal to one: true amplification is never possible in this case.

References

- Andrews, R W, Peterson, R W, Purdy, T P, Cicak, K, Simmonds, R W, Regal, C A, and Lehnert, K W (2014, March). Bidirectional and efficient conversion between microwave and optical light. *Nat. Phys.*, **10**(4), 321–326.
- Aspelmeyer, Markus, Kippenberg, Tobias J., and Marquardt, Florian (2014, Dec). Cavity optomechanics. *Rev. Mod. Phys.*, **86**, 1391–1452.
- Averin, D. (2003). Linear quantum measurements. In *Quantum Noise in Mesoscopic Systems* (ed. Y. Nazarov), pp. 205–228. Kluwer, Amsterdam.
- Bocko, Mark F. and Onofrio, Roberto (1996). On the measurement of a weak classical force coupled to a harmonic oscillator: experimental progress. *Rev. Mod. Phys.*, **68**, 755–799.
- Braginsky, V. B. and Khalili, F. Y. (1992). *Quantum Measurement*. Cambridge University Press, Cambridge.
- Braginsky, V. B. and Khalili, F. Y. (1996). Quantum nondemolition measurements: the route from toys to tools. *Rev. Mod. Phys.*, **68**, 1.
- Braginsky, V. B., Vorontsov, Y. I., and Thorne, K. P. (1980). Quantum nondemolition measurements. *Science*, **209**, 547–557.
- Bruus, Henrik and Flensberg, Karsten (2004). *Many-body quantum theory in condensed matter physics: a introduction*. Oxford University Press, Oxford.
- Caves, C.M. and Milburn, G J (1987). Quantum-Mechanical Model for Continuous Position Measurements. *Phys. Rev. A*, **36**(12), 5543–5555.
- Caves, Carlton M. (1981). Quantum-mechanical noise in an interferometer. *Phys. Rev. D*, **23**, 1693–1708.
- Caves, Carlton M., Thorne, Kip S., Drever, Ronald W. P., Sandberg, Vernon D., and Zimmermann, Mark (1980). On the measurement of a weak classical force coupled to a quantum-mechanical oscillator. i. issues of principle. *Rev. Mod. Phys.*, **52**, 341–392.
- Clerk, A. A. (2004). Quantum-limited position detection and amplification: A linear response perspective. *Phys. Rev. B*, **70**, 245306.
- Clerk, A. A., Devoret, M. H., Girvin, S. M., Marquardt, F., and Schoelkopf, R. J. (2010). Introduction to quantum noise, measurement and amplification. *Rev. Mod. Phys.*, **82**, 1155.
- Clerk, A A and Marquardt, F. (2014). *Cavity Optomechanics*, Chapter Basic Theory of Cavity Optomechanics, pp. 5–23. Springer, Berlin.
- Clerk, A. A., Marquardt, F., and Jacobs, K. (2008). Back-action evasion and squeezing of a mechanical resonator using a cavity detector. *New J. Phys.*, **10**, 095010.
- Dong, C, Fiore, V, Kuzyk, M C, and Wang, H (2012, December). Optomechanical Dark Mode. *Science*, **338**(6114), 1609–1613.
- Gerry, C. and Knight, P. (2005). *Introductory Quantum Optics*. Cambridge University

- Press, Cambridge.
- Gottfried, K. (1966). *Quantum Mechanics, Volume I: Fundamentals*. W. A. Benjamin, Inc.
- Hertzberg, J. B., Rocheleau, T., Ndukum, T., Savva, M., Clerk, A. A., and Schwab, K. C. (2010). Back-action evading measurements of nanomechanical motion. *Nature Phys.*, **6**, 213.
- Hill, Jeff T, Safavi-Naeini, Amir H, Chan, Jasper, and Painter, Oskar (2012, October). Coherent optical wavelength conversion via cavity optomechanics. *Nat. Comm.*, **3**, 1196–7.
- Jacobs, K. (2010). *Stochastic Processes for Physicists*. Cambridge University Press, Cambridge.
- Jacobs, Kurt (2014). *Quantum Measurement Theory and its Applications*. Cambridge University Press, Cambridge.
- Jacobs, K. and Steck, D. A. (2006). A straightforward introduction to continuous quantum measurement. *Contemporary Physics*, **47**, 279.
- Khalili, Farid, Miao, Haixing, Yang, Huan, Safavi-Naeini, Amir H, Painter, Oskar, and Chen, Yanbei (2012, September). Quantum back-action in measurements of zero-point mechanical oscillations. *Phys. Rev. A*, **86**(3), 033840.
- Kronwald, Andreas, Marquardt, Florian, and Clerk, Aashish A. (2013, Dec). Arbitrarily large steady-state bosonic squeezing via dissipation. *Phys. Rev. A*, **88**, 063833.
- Law, C. K. (1995, March). Interaction between a moving mirror and radiation pressure: A Hamiltonian formulation. *Phys. Rev. A*, **51**(3), 2537–2541.
- Lecocq, F, Clark, J B, Simmonds, R W, Aumentado, J, and Teufel, J D (2015, December). Quantum Nondemolition Measurement of a Nonclassical State of a Massive Object. *Phys. Rev. X*, **5**(4), 041037.
- Lemondé, Marc-Antoine and Clerk, Aashish A. (2015, Mar). Real photons from vacuum fluctuations in optomechanics: The role of polariton interactions. *Phys. Rev. A*, **91**, 033836.
- Marquardt, F., Chen, J. P., Clerk, A. A., and Girvin, S. M. (2007). Quantum theory of cavity-assisted sideband cooling of mechanical motion. *Phys. Rev. Lett.*, **99**, 093902.
- Pace, A F, Collett, M J, and Walls, D F (1993, April). Quantum Limits in Interferometric Detection of Gravitational-Radiation. *Phys. Rev. A*, **47**(4), 3173–3189.
- Pirkkalainen, J.-M., Damskäg, E., Brandt, M., Massel, F., and Sillanpää, M. A. (2015, Dec). Squeezing of quantum noise of motion in a micromechanical resonator. *Phys. Rev. Lett.*, **115**, 243601.
- Suh, J, Weinstein, A J, Lei, C U, Wollman, E E, Steinke, S K, Meystre, P, Clerk, Aashish, and Schwab, K. C. (2014, June). Mechanically detecting and avoiding the quantum fluctuations of a microwave field. *Science*, **344**(6189), 1262–1265.
- Tsang, Mankei and Caves, Carlton M. (2010, Sep). Coherent quantum-noise cancellation for optomechanical sensors. *Phys. Rev. Lett.*, **105**, 123601.
- Vyatchanin, S.P. and Zubova, E.A. (1995). Quantum variation measurement of a force. *Physics Letters A*, **201**(4), 269 – 274.
- Vyatchanin, S. P. and Matsko, A. B. (1996). Quantum variational measurements of force and compensation of the nonlinear backaction in an interferometric displace-

- ment transducer. *JETP*, **83**(4), 690.
- Walls, D. F. and Milburn, G. J. (2008). *Quantum Optics* (2nd edn). Springer, Berlin.
- Wasilewski, W., Jensen, K., Krauter, H., Renema, J. J., Balabas, M. V., and Polzik, E. S. (2010, Mar). Quantum noise limited and entanglement-assisted magnetometry. *Phys. Rev. Lett.*, **104**, 133601.
- Wilson-Rae, I., Nooshi, N., Zwerger, W., and Kippenberg, T. J. (2007). Theory of ground state cooling of a mechanical oscillator using dynamical back-action. *Phys. Rev. Lett.*, **99**, 093901.
- Wiseman, H. M. and Milburn, G. J. (2014). *Quantum Measurement and Control*. Cambridge University Press, Cambridge.
- Wollman, E. E., Lei, C. U., Weinstein, A. J., Suh, J., Kronwald, A., Marquardt, F., Clerk, A. A., and Schwab, K. C. (2015). Quantum squeezing of motion in a mechanical resonator. *Science*, **349**(6251), 952–955.
- Woolley, M. J. and Clerk, A. A. (2013, Jun). Two-mode back-action-evading measurements in cavity optomechanics. *Phys. Rev. A*, **87**, 063846.
- Woolley, M. J. and Clerk, A. A. (2014, Jun). Two-mode squeezed states in cavity optomechanics via engineering of a single reservoir. *Phys. Rev. A*, **89**, 063805.